



*Citation for published version:*

Darnell, R, Nakatani, Y, Knottenbelt, M, Gebhard, S & Cook, GM 2019, 'Functional characterization of BcrR: a one-component transmembrane signal transduction system for bacitracin resistance', *Microbiology*, vol. 165, no. 4, pp. 475-487. <https://doi.org/10.1099/mic.0.000781>

*DOI:*

[10.1099/mic.0.000781](https://doi.org/10.1099/mic.0.000781)

*Publication date:*

2019

*Document Version*

Peer reviewed version

[Link to publication](#)

© R. Darnell, Y. Nakatani, M. Knottenbelt, S. Gebhard, and G. Cook, 2019. The definitive peer reviewed, edited version of this article is published in *Microbiology*, Volume 165, 2019, DOI 10.1099/mic.0.000781

## University of Bath

### General rights

Copyright and moral rights for the publications made accessible in the public portal are retained by the authors and/or other copyright owners and it is a condition of accessing publications that users recognise and abide by the legal requirements associated with these rights.

### Take down policy

If you believe that this document breaches copyright please contact us providing details, and we will remove access to the work immediately and investigate your claim.

1 **Revised Ms. No. MIC-D-18-00158**  
2 **Functional Characterisation of BcrR: A One-Component Transmembrane**  
3 **Signal Transduction System for Bacitracin Resistance**

4  
5 **Rachel L. Darnell<sup>1,2</sup>, Yoshio Nakatani<sup>1,2</sup>, Melanie K Knottenbelt<sup>1</sup>, Susanne**  
6 **Gebhard<sup>3</sup>, and Gregory M. Cook<sup>1,2\*</sup>**

7  
8 <sup>1</sup>Department of Microbiology and Immunology, University of Otago, Dunedin, New  
9 Zealand

10 <sup>2</sup>Maurice Wilkins Centre for Molecular Biodiscovery, The University of Auckland,  
11 Private Bag 92019, Auckland 1042, New Zealand

12 <sup>3</sup>Milner Centre for Evolution, Department of Biology and Biochemistry, University of  
13 Bath, UK

14

15 For correspondence (Gregory M Cook) Email: greg.cook@otago.ac.nz; Tel: +64 3  
16 4797722

17

18 **Keywords:** *Enterococcus*, antimicrobial resistance, membrane protein, regulator

19 **Subject category:** Regulation

20 **Word Count:** 5,433<sup>i</sup>

21

---

<sup>i</sup> Abbreviations: ABC ATP-binding cassette; DDM *n*-dodecyl- $\beta$ -D-maltoside, EMSA electrophoretic mobility shift assays; GOF gain of function; HA hydroxylamine hydrochloride; *lacZ*  $\beta$ -galactosidase; LB lysogeny broth; LOF loss of function; *luxABCDE* luciferase; MUG 4-methylumbelliferyl  $\beta$ -D-galactoside; NC negative control; P<sub>bcrA</sub> bcrA promoter; WT wild-type

## 22 Abstract

23 Bacitracin is a cell wall targeting antimicrobial with clinical and agricultural  
24 applications. With the growing mismatch between antimicrobial resistance and  
25 development, it is essential we understand the molecular mechanisms of  
26 resistance in order to prioritise and generate new effective antimicrobials. BcrR  
27 is a unique membrane-bound one-component system that regulates high-level  
28 bacitracin resistance in *Enterococcus faecalis*. In the presence of bacitracin,  
29 BcrR activates transcription of the *bcrABD* operon conferring resistance  
30 through a putative ATP-binding cassette (ABC) transporter (BcrAB). BcrR has  
31 three putative functional domains, a N-terminal helix-turn-helix DNA-binding  
32 domain, an intermediate oligomerisation domain, and a C-terminal  
33 transmembrane domain. However, the molecular mechanisms of signal  
34 transduction remain unknown. Random mutagenesis of *bcrR* was performed to  
35 generate loss and gain of function mutants using transcriptional reporters fused  
36 to the target promoter  $P_{bcrA}$ . Fifteen unique mutants were isolated across all  
37 three proposed functional domains, comprising fourteen loss of function and  
38 one gain of function. The gain of function variant (G64D) mapped to the putative  
39 dimerisation domain of BcrR, and functional analyses indicated that the G64D  
40 mutant constitutively expresses the  $P_{bcrA}$ -*luxABCDE* reporter. DNA-binding and  
41 membrane insertion were not affected in the five mutants chosen for further  
42 characterisation. Homology modelling revealed putative roles for two key  
43 residues (R11 and S33) in BcrR activation. Here we present a new model of BcrR  
44 activation and signal transduction, providing valuable insight into the functional  
45 characterisation of membrane-bound one-component systems and how they  
46 can co-ordinate critical bacterial responses, such as antimicrobial resistance.

## 47 INTRODUCTION

48 One-component regulatory systems containing both a sensory domain and DNA-  
49 binding domain dominate signal transduction systems in bacteria and archaea [1].  
50 They regulate important cellular functions such as antimicrobial resistance, metal  
51 homeostasis, carbon and amino acid metabolism, and quorum sensing [2]. They are  
52 both evolutionarily older and more widely distributed than their two-component  
53 counterparts [1, 2]. However, they are vastly understudied, particularly those that are  
54 membrane-bound [1].

55 BcrR is a unique one-component regulator of high-level zinc-bacitracin (bacitracin)  
56 resistance in *Enterococcus faecalis* [3]. BcrR consists of three proposed functional  
57 domains, a N-terminal helix-turn-helix (HTH) DNA-binding domain, an intermediate  
58 oligomerisation domain and a C-terminal transmembrane domain [4]. We have  
59 previously shown BcrR directly detects bacitracin *in vitro* [5]. Intrinsic tryptophan  
60 fluorescence of BcrR was reduced in the presence of bacitracin, suggesting a direct  
61 interaction between BcrR and bacitracin [5]. Previous electrophoretic mobility shift  
62 assays (EMSAs) and  $P_{bcrA}$ -*lacZ* reporter assays have shown that BcrR is constitutively  
63 bound to two sets of inverted DNA repeat sequences upstream of its resistance  
64 operon, *bcrABD*, but requires bacitracin for activation [4]. BcrR is therefore thought to  
65 exist as dimers in its inactive state, with oligomerisation (likely dimer-dimer formation)  
66 induced upon addition of bacitracin. The DNA-binding footprint of BcrR on the *bcrABD*  
67 promoter region does not change between induced and uninduced states, suggesting  
68 a conformational change in BcrR, and/or subtle changes in local DNA topology are  
69 required to initiate *bcrABD* expression [5]. How BcrR binds bacitracin and transduces  
70 the signal to initiate *bcrABD* expression remains unknown.

71 The first two genes in the target operon, *bcrAB*, encode a putative heterodimeric ABC  
72 efflux transporter (BcrAB) that is essential for high-level bacitracin resistance [3]. This  
73 transporter is distinct from other ABC transporters (i.e. BceAB) that are frequently  
74 associated with drug removal in Firmicute bacteria, such as *Enterococcus* and  
75 *Bacillus* [3, 6–8], in that its expression is regulated by a one-component rather than  
76 two-component system [8–10]. The third target gene, *bcrD*, encodes an  
77 uncharacterised undecaprenyl pyrophosphate phosphatase that is not necessary for  
78 high-level resistance [3].

79 The aim of this study was to identify key residues critical for BcrR function using  
80 random mutagenesis and reporter assays, to further our understanding of the role  
81 these three functional domains play in one-component signal transduction systems.  
82 Fifteen unique mutations were identified, fourteen loss of function (LOF) and one gain  
83 of function (GOF). The G64D GOF mutant was localised to the putative dimerisation  
84 domain of BcrR. The transcription activation profile of the GOF G64D mutant was  
85 determined using the  $P_{bcrA}$ -*luxABCDE* reporter in order to understand its ability to  
86 activate *bcrABD* in the absence of the inducer, bacitracin. A further four mutants (in  
87 addition to G64D) spanning all three functional domains were chosen for detailed  
88 characterisation of cellular localisation and DNA-binding capability. A three-  
89 dimensional model was constructed of the DNA-binding domain (DBD) to further  
90 elucidate the role of the DBD mutants in BcrR function.

## 91 **METHODS**

### 92 **Bacterial strains and growth conditions**

93 All strains used in this study are listed in Table S1, the *Bacillus subtilis* SGB37 strain  
94 was used as a heterologous host for transformation and expression of mutant *bcrR*,

95 and BcrR activity assays. Genomic DNA was isolated from the *E. faecalis* strain  
96 AR01/DGVS and used as a template for PCR amplification of *bcrR*. *Escherichia coli*  
97 strains DH10B and C41(DE3) were used for cloning and protein production,  
98 respectively. *E. coli* and *B. subtilis* were routinely grown in lysogenic broth (LB) media  
99 at 37°C overnight (200 r.p.m), while *E. faecalis* was grown in brain heart infusion (BHI)  
100 media at 37°C with no agitation. For protein production, *E. coli* C41(DE3) was grown  
101 in 2 × yeast extract and tryptone (2 × YT) at 37°C (200 r.p.m), unless otherwise stated.  
102 *B. subtilis* was transformed by natural competence as previously described [11].  
103 Selective media contained ampicillin (amp; 100 µg ml<sup>-1</sup> for *E. coli*), chloramphenicol  
104 (cm; 5 µg ml<sup>-1</sup> for *B. subtilis*), kanamycin (kan; 10 µg ml<sup>-1</sup> for *B. subtilis*), and  
105 spectinomycin (spec; 100 µg ml<sup>-1</sup> for *B. subtilis*), where required. Bacitracin (bac; 0.5  
106 µg ml<sup>-1</sup> for *B. subtilis*), xylose (xyl; 0.2% (w/v) for *B. subtilis*), and 5-bromo-4-chloro-3-  
107 indolyl β-D-galactopyranoside (X-gal; 100 µg ml<sup>-1</sup> for *B. subtilis*) were added to LB agar  
108 to select for LOF and GOF *bcrR* mutants. All solid media contained 1.5% (w/v) agar.  
109 Growth was measured as an optical density at 600 nm (OD<sub>600</sub>) (Jenway 6300  
110 Spectrophotometer).

### 111 **Hydroxylamine mutagenesis of *bcrR***

112 Full length *bcrR* was previously cloned into the xylose-inducible plasmid pES701 (pXT-  
113 *bcrR*) (Table S1) [12]. The pXT-*bcrR* plasmid was randomly mutagenised by  
114 incubation with the chemical mutagen hydroxylamine hydrochloride (HA) (1.25 mg per  
115 µg of DNA) in sodium phosphate buffer (f/c 50 mM sodium phosphate pH 7.0, 100 mM  
116 NaCl, 25 mM EDTA) at 75°C for 15 min (Fig. 1). Mutated pXT-*bcrR* (mut*bcrR*) plasmid  
117 was purified by gel electrophoresis purification using the illustra™ GFX™ PCR DNA  
118 and gel band purification kit (GE Healthcare) (Table S1). The plasmid mut*bcrR* was  
119 used to transform *B. subtilis* strain SGB37 (harbouring P<sub>*bcrA*</sub>-*lacZ*) and *B. subtilis* strain

120 SGB273 (harbouring  $P_{bcrA}$ -*luxABCDE*), plated on LB<sub>spec</sub> agar and screened for LOF or  
121 GOF [11].

### 122 **Isolation of LOF and GOF *bcrR* mutants**

123 A modified protocol of traditional blue-white screening was used to isolate colonies  
124 with BcrR LOF or GOF [12]. LOF mutants were identified as white colonies on  
125 LB<sub>bac,xyl,Xgal</sub> agar plates (i.e. white = LOF), due to their inability to produce active BcrR,  
126 and are therefore unable to initiate expression of the  $\beta$ -galactosidase reporter  
127 construct  $P_{bcrA}$ -*lacZ* (Fig. 1 and Fig. S1). GOF mutants were identified as blue colonies  
128 on LB<sub>xyl/Xgal</sub> plates, due to their ability to produce active BcrR in the absence of its  
129 inducer (bacitracin) and subsequently initiate expression of the  $\beta$ -galactosidase (Fig.  
130 1 and Fig. S1). GOF mutants were also identified as luminescing colonies on LB<sub>xyl</sub>  
131 agar plates in a SGB273 background. Mutations in putative LOF and GOF mutants  
132 were verified by DNA sequencing using the primer pair pXT-check fwd and pXT-check  
133 rev (Table S2).

### 134 **$\beta$ -galactosidase and luciferase assays**

135  $\beta$ -galactosidase assays using the fluorogenic substrate 4-methylumbelliferyl  $\beta$ -D-  
136 galactoside (MUG) were carried out on all integrative *lacZ* reporter strains to  
137 quantitatively verify BcrR loss and gain of function phenotypes. BcrR mutant and  
138 control strains were grown to an OD<sub>600</sub> of 0.4 in LB broth containing 0.2% xylose.  
139 Samples (100  $\mu$ l) were taken and placed in four wells of a 96-well microtitre plate for  
140 each replicate of each strain. Cultures were challenged with 0, 0.1, 0.5, and 1  $\mu$ g ml<sup>-1</sup>  
141 of bacitracin for 1 h. Cell density was determined as a final OD<sub>600</sub> using the Varioskan  
142 Flash Multimode Reader (Thermo Fisher Scientific) and plates were subsequently  
143 frozen at - 80°C. Expression analysis was measured as previously described [12, 13].

144 An unpaired *t*-test was performed between the wild-type (WT) and vector control (NC),  
145 along with the WT and BcrR mutants at 1  $\mu\text{g ml}^{-1}$  bacitracin to determine statistical  
146 significance of respective  $\beta$ -galactosidase activities (an adjusted *p* value of  $\leq 0.05$ ).

147 Luciferase activities of WT and G64D mutant BcrR were assayed using a Varioskan  
148 Flash Multimode Reader (Thermo Fisher Scientific) as previously described, with the  
149 following modifications [12]. Cultures were grown in the presence or absence of xylose  
150 (0.2%) to an OD<sub>600</sub> of 0.1 and plated onto a 96-well microtitre plate. Cultures were  
151 challenged with final bacitracin concentrations of 0, 0.1, 0.5, and 1  $\mu\text{g ml}^{-1}$  for 2 h, with  
152 OD<sub>600</sub> and luminescence measured every 20 min.

### 153 **Generation of wild-type and mutant BcrR protein expression constructs**

154 Wild-type BcrR and five BcrR mutants (R11K, S33L, G64D, E179K, and T183M) were  
155 selected for further investigation. BcrRFwd and HisBcrRRev primers were used to  
156 clone WT *bcrR* from *E. faecalis* strain AR01/DGVS into the IPTG-inducible expression  
157 vector pTrc99A to produce pBcrRHis<sup>WT</sup> (Table S1 and S2). A His<sub>6</sub> tag was introduced  
158 at the C-terminus of BcrR for purification purposes. Respective mutations for each  
159 selected mutant were introduced into WT *bcrR* using site-directed mutagenesis and  
160 overlap extension PCR to create the five BcrR variants pBcrRHis<sup>R11K</sup>, pBcrRHis<sup>S33L</sup>,  
161 pBcrRHis<sup>G64D</sup>, pBcrRHis<sup>E179K</sup>, pBcrRHis<sup>T183M</sup> (Tables S1 and S2) [14]. Constructs were  
162 confirmed by DNA sequencing. Chemically competent *E. coli* C41(DE3) were  
163 transformed (by heat-shock) with pBcrRHis<sup>WT</sup> and mutant plasmids, to generate  
164 strains WT, R11K, S33L, G64D, E179K, and T183M for protein production and  
165 purification (Table S1).

### 166 **Cellular localisation of BcrR wild-type and mutant forms**



167 *E. coli* strains producing BcrR WT and BcrR mutant protein were grown in 2 × YT<sub>amp</sub>  
168 media. When cultures reached an OD<sub>600</sub> of 0.6 – 0.8 expression was induced with 1  
169 mM IPTG and cells were grown for a further 2 h. Cells were harvested by low-speed  
170 centrifugation (15 min, 10,000 × *g* at 4°C) and resuspended in lysis buffer (50 mM  
171 Tris/HCl, 5 mM MgCl<sub>2</sub>, pH 7.5). Cells were lysed by three passages through the  
172 Aminco French Press at 40 kpsi at 4°C. Unbroken cells and debris were removed by  
173 low speed centrifugation (15 min, 10,000 × *g* at 4°C) and the cell lysate underwent  
174 high speed centrifugation (90 min, 123,695 × *g* at 4°C) to separate the membrane and  
175 cytosolic fractions. Supernatants were removed, and membrane pellets were  
176 resuspended in lysis buffer, both were stored at -20°C.

177 Protein concentrations in the cytoplasmic and membrane fractions were determined  
178 by DC Bradford (BioRad) using bovine serum albumin (BSA) as a standard. Protein  
179 samples (about 50 µg) of both membrane and cytoplasmic fractions were run on  
180 12.5% SDS-PAGE gel, 125 V for 1.5 h using the Laemmli-SDS buffering system, and  
181 protein was visualised by standard silver staining [15]. Western Blot analysis was used  
182 to confirm BcrRHis WT and BcrR mutant protein was the ~20 kDa protein observed in  
183 the membrane fraction. Western Blots were carried out using a previously described  
184 protocol with an anti-His antibody (Abcam ab1187) and visualised using the Odyssey  
185 Fc Imaging System (LI-COR® Biosciences) [4].

#### 186 **Protein purification of WT and mutant BcrRHis, and reconstitution into** 187 **liposomes**

188 All six BcrR variants underwent protein purification using a previously described  
189 method with the following modifications [4]. Overproduction of BcrR is toxic to *E. coli*,  
190 therefore to optimise protein yield, 750 ml *E. coli* cultures were grown in 2 L flasks in

191 2 × YT media, supplemented with ampicillin, with agitation and aeration (200 r.p.m) at  
192 37°C [4]. At OD<sub>600</sub> 1.5 - 2, the cultures were induced with 1 mM IPTG and incubated  
193 for a further 1 h. Cells were lysed by two passages through the Constant Systems Ltd  
194 Cell Disrupter at 31 kpsi and 4°C. Membranes were stored at - 20°C for BcrR  
195 solubilisation and purification the following day. Prior to solubilisation, membranes  
196 were washed with buffer A (20 mM sodium phosphate pH 7.5, 0.1 mM PMSF, 5 mM  
197 DTT, 500 mM sodium chloride) containing 0.5% sodium cholate and disrupted by  
198 sonication (20% Amp) on ice for 6 × 30 sec cycles with 1 min rest periods. Membranes  
199 were ultra-centrifuged at 150,000 × *g* for 45 min. Membranes were then solubilised  
200 with buffer A containing 1% *n*-dodecyl-β-D-maltoside (DDM) and disrupted by  
201 sonication (as above). Solubilised protein was ultra-centrifuged at 150,000 × *g* for 45  
202 min. The supernatant (solubilised BcrR) was stored on ice and solubilisation was  
203 repeated for optimal protein yield. The supernatant was loaded onto a Ni<sup>2+</sup> HisTrap  
204 HP column (5 ml) using an AKTA Prime Plus (GE Healthcare) pre-equilibrated with  
205 five column volumes of buffer A containing 0.5% DDM and 10% glycerol (buffer A\*  
206 Unbound sample was removed by washing with buffer A\* and buffer B (buffer A\*  
207 containing 500 mM imidazole) at a ratio of 80:20 (at a rate of 2 ml min<sup>-1</sup>). BcrRHis was  
208 eluted (at a rate of 1 ml min<sup>-1</sup>) at a buffer A\*- buffer B ratio of 30:70 and collected in  
209 1ml fractions. Remaining protein was eluted in 100% buffer B. In all cases elution was  
210 monitored by absorption at 280 nm in Primeview. Fractions collected from the 30:70  
211 peak were analysed by SDS-PAGE and visualised with Coomassie G-250 (Bio-Rad)  
212 (Fig. S2. a - f). BcrR-containing fractions were pooled and placed in Snakeskin®  
213 Pleated Dialysis Tubing (3,500 MWCO) and dialysed in 100 volumes of buffer A  
214 containing 10% glycerol at 4°C overnight with gentle stirring. Dialysed protein was

215 analysed by SDS-PAGE and protein was quantified by DC Bradford (BioRad) using a  
216 BSA standard. Average final protein concentrations were 3.5 - 5 mg ml<sup>-1</sup>.

217 BcrRHis WT and mutants were reconstituted into L- $\alpha$ -phosphotidyl-choline liposomes  
218 (Sigma P5638) for electrophoretic mobility shift assays. BcrRHis WT and mutant  
219 protein was added to lipid at a ratio of 1:20 (protein:lipid), Triton X-100 and BioBeads®  
220 (BioRad) were used to integrate BcrRHis into liposomes to create BcrRHis WT, R11K,  
221 S33L, G64D, E179K, and T183M proteoliposomes using a previously reported  
222 protocol [5]. Protein concentration was quantified by separating protein from lipid on a  
223 12.5% SDS-PAGE gel containing four times the normal amount of SDS, alongside a  
224 BSA protein standard (Fig. S3).

### 225 **Electrophoretic Mobility Shift Assays (EMSA)**

226 EMSAs were used to determine DNA-binding capacity of each of the five BcrRHis  
227 variants to the  $P_{bcrA}$  target promoter.  $P_{bcrA}$  was amplified by PCR, using primers  
228 bcrA\_EMSA\_F and bcrA\_EMSA\_R to produce a 92 bp DNA probe. The forward  
229 primer, bcrA\_EMSA\_F was tagged at the 5' end with a 5'IRDye700 fluorophore (LI-  
230 COR® Biosciences/Integrated DNA Technologies) for visualisation at 700 nm (Table  
231 S2). Non-labelled competitor probe was amplified by PCR, using the primers  
232 bcrA\_EMSA\_F (without the IRDye700 label) and bcrA\_EMSA\_R (Table S2). Binding  
233 reactions were carried out using a previously described method with the following  
234 modifications: 1.9 ng (32 fmoles) of labelled DNA was used in all binding reactions,  
235 and reactions were carried out at molar ratios of BcrR:DNA (0:1, 25:1, 50:1, and  
236 125:1) in the dark, at room temperature [4]. Reactions were run on pre-cooled and  
237 pre-run (120 V, 1 h) 6% native acrylamide gels (37.5:1 acrylamide:bisacrylamide) in  
238 0.5 TBE (40 mM Tris-HCl (pH 8.3), 45 mM boric acid, 1 mM EDTA) on ice in a dark

239 room at 350 V for 25 min. Gels were visualised for 10 min at 700 nm using the  
240 Odyssey® Fc Imaging System (LI-COR® Biosciences) with minimum light exposure.

### 241 **BcrR three-dimensional structural model**

242 A three-dimensional model of the BcrR DNA-binding domain was predicted using the  
243 P22 c2 repressor protein, which has the highest homology to BcrR (34% identity) (PDB  
244 file: 3JXB), as a model in ProtMod (Godzik Lab, The Burnham Institute). Structural  
245 analysis and amino acid substitution was carried out using PyMOL (The PyMOL  
246 Molecular Graphics System, Version 1.7 Schrödinger, LLC) [16].

## 247 **RESULTS AND DISCUSSION**

### 248 **Isolation and characterisation of loss and gain of function mutations in BcrR**

249 Loss (LOF) and gain of function (GOF) BcrR mutants were identified using *B. subtilis*  
250 strain SGB37 as a heterologous host as previously described [12]. Mutant BcrR  
251 (*mutbcrR*) was integrated into the host genome alongside the reporter for BcrR activity  
252  $P_{bcrA}$ -*lacZ* ( $\beta$ -galactosidase), following successful transformation. LOF and GOF  
253 mutants were isolated using a modified blue-white screening protocol as previously  
254 described [12]. LOF mutants were white in the presence of bacitracin, due to their  
255 inability to activate  $P_{bcrA}$ -*lacZ* expression, while GOF mutants were identified as blue  
256 colonies in the absence of bacitracin due to their ability to activate  $P_{bcrA}$ -*lacZ*  
257 expression in the absence of bacitracin (Fig. 1 and Fig. S1).

258 A total of 428 colonies were screened for loss and gain of BcrR function. The average  
259 loss of function frequency was 8.3% (data not shown). All loss and gain of function  
260 mutants were sequenced to identify point mutations responsible for their respective  
261 phenotype. A total of fifteen unique *bcrR* point mutants were isolated using the  $\beta$ -  
262 galactosidase reporter (Table 1). Mapping to the BcrR protein sequence identified four

263 substitutions in the predicted helix-turn-helix (HTH) DNA-binding domain (DBD) motif  
264 (R11K, T17M, T30I, and S33L), four in the putative oligomerisation domain (OGD)  
265 (P42L, S51F, G64S, and G64D), and seven in the transmembrane domain (TMD) –  
266 four in the putative first and second transmembrane helices (G88R, P101L, T123I, and  
267 G141D), and three in the second extracellular loop (E179K, P180S, and T183M) (Fig.  
268 2). A number of mutations were observed more than once, and all mutations conferred  
269 a LOF, except G64D which resulted in a GOF (Table 1). Only one GOF mutant was  
270 isolated using the luciferase reporter ( $P_{bcrA}$ -*luxABCDE*). Coincidentally, this mutant  
271 carried the same G64D substitution as the  $\beta$ -galactosidase GOF mutant.

### 272 **Quantitative measurement and validation of BcrR mutant activity**

273 BcrR activity in each of the LOF and GOF mutants was quantitatively measured using  
274  $\beta$ -galactosidase assays (Fig. 3). Fluorescence (MUG) emitted by  $\beta$ -galactosidase  
275 activity was measured for each mutant at a range of bacitracin concentrations (0, 0.1,  
276 0.5 and 1  $\mu\text{g ml}^{-1}$ ) and compared to the BcrR wild-type (WT) and empty vector control  
277 (NC). All strains were grown in the presence of xylose (0.2%) to ensure *bcrR*  
278 expression. WT BcrR activity ( $P_{bcrA}$ -*lacZ* expression) was dose-dependent and  
279 maximal activity was observed at 1  $\mu\text{g ml}^{-1}$  bacitracin (2000 RFU) (Fig. 3). The vector  
280 control showed a negligible response with a maximal activity of 20 RFU (Fig. 3).  
281 Thirteen of the fourteen LOF mutants from all three protein domains showed similar  
282 activity to the vector control, validating their LOF phenotype (Fig. 3). The G64S mutant  
283 displayed higher activity than the rest of the LOF mutants but remained significantly  
284 lower than WT in the presence of bacitracin, and therefore remained classified as LOF  
285 (Fig. 3b). Interestingly, the GOF mutant (G64D) was still inducible by bacitracin and  
286 expression was 3-fold higher than the WT at 1  $\mu\text{g ml}^{-1}$  bacitracin (Fig. 3b).

287 To validate the genomic-phenotypic linkages of the BcrR point mutations, genomic  
288 DNA (gDNA) was isolated from three LOF BcrR mutant *B. subtilis* strains (S33L,  
289 G64S, and E179K), the GOF mutant (G64D) strain, and the WT strain (SGB43) (Table  
290 1 and Table S1) using a previously described protocol [11]. This was to provide a  
291 “clean” genetic background, and to absolve any chance the observed LOF phenotype  
292 was due to a loss of  $\beta$ -galactosidase activity, rather than the associated BcrR point  
293 mutation. Clonal cultures of the *B. subtilis*  $P_{bcrA}$ -*lacZ* reporter strain (SGB37; Table S1)  
294 were independently transformed with gDNA from each of the stated strains.  
295 Transformants were plated on LB agar containing spectinomycin to select for uptake  
296 of the BcrR construct. Three clones for each BcrR variant were streaked on LB<sub>xyI,bac,Xgal</sub>  
297 agar to phenotypically confirm BcrR function (Fig. S1). BcrR presence was detected  
298 in all clones by colony PCR. The G64D GOF mutant appeared as blue colonies, which  
299 represents activated BcrR and are darker than the light blue WT, indicating an  
300 increased activation state in the G64D mutant (Fig. S1a – b). The colonies for the LOF  
301 mutants S33L, G64S, and E179K (Fig. S1c - e), appeared white in colour, which  
302 represents a lack of active BcrR, i.e. LOF. BcrR activity was quantified for each BcrR  
303 variant by  $\beta$ -galactosidase activity analysis using the fluorogenic substrate MUG.  
304 Activity for each BcrR variant was comparable to the original assay (Fig. 3 and Fig.  
305 S4). This suggests these are indeed bona fide loss and gain of function BcrR point  
306 mutations, further supported by the independent isolation of most point mutations on  
307 more than one occasion (see “Frequency” Table 1).

### 308 **The bacitracin activation profile of the BcrR gain of function mutant G64D**

309 Two substitutions were observed at the same residue G64 (S and D), resulting in both  
310 a LOF and GOF genotype respectively. This residue is localised to the putative  
311 oligomerisation domain of BcrR, and oligomeric state is believed to play an important

312 role in BcrR activation [5]. The *bcrA* promoter consists of two sets of inverted repeats  
313 that are essential for BcrR binding, and BcrR is often observed in both the monomeric  
314 and dimeric form [4]. Previous findings suggest BcrR forms a tetrameric dimer-dimer  
315 complex upon activation by bacitracin, therefore we hypothesise G64 may play a  
316 critical role in the formation of this complex [4, 5]. To investigate this proposal further,  
317 we carried out a more detailed analysis of the G64D activation profile (Fig. 4).

318 BcrR G64D activity was compared to WT BcrR using the integrative luciferase reporter  
319 construct  $P_{bcrA}$ -*luxABCDE* in the *B. subtilis* strain SGB273. Luciferase activity was  
320 used in place of  $\beta$ -galactosidase due to its greater sensitivity to activated BcrR (as  
321 observed in the absence of bacitracin, Fig. 3b and 4a). A comparison of BcrR WT and  
322 G64D activity was carried out in the presence of xylose (0.2%) and at a range of  
323 bacitracin concentrations (0, 0.1, 0.5 and 1  $\mu\text{g ml}^{-1}$ ). BcrR G64D activity was  
324 significantly higher than WT at 0 and 0.1  $\mu\text{g ml}^{-1}$  of bacitracin (Fig. 4a and 4b), but  
325 there was no significant difference at 0.5 and 1  $\mu\text{g ml}^{-1}$  of bacitracin (Fig. 4c and 4d).  
326 We hypothesise the G64D mutation stabilises BcrR at 0 and 0.1  $\mu\text{g ml}^{-1}$  of bacitracin  
327 allowing for spontaneous activation and hyper-sensitivity upon addition of low levels  
328 of bacitracin, while WT requires bacitracin for activation. It is also likely that binding of  
329 bacitracin stabilises BcrR, and this may explain why we do not see a significant  
330 difference in G64D and WT activity at 0.5 and 1  $\mu\text{g ml}^{-1}$  of bacitracin.

331 In the *B. subtilis* heterologous host strains, BcrR expression in the integrative pXT-  
332 *bcrR* plasmid is under the control of a xylose-inducible promoter cloned upstream of  
333 the *bcrR* gene. However, this promoter is known to be leaky [17]. Therefore, to ensure  
334 the observed G64D phenotype was not an artefact of high BcrR expression and to  
335 mimic low-level constitutive BcrR expression as observed in its native enterococcal  
336 environment [3], luciferase assays were repeated in the absence of xylose. This

337 showed G64D activity was also significantly higher than WT at 0 and 0.1  $\mu\text{g ml}^{-1}$  of  
338 bacitracin, but not at 0.5 or 1  $\mu\text{g ml}^{-1}$  at low levels of BcrR expression (albeit at lower  
339 overall levels) (Fig. 5 a – d). This suggests the G64D mutation is of physiological  
340 significance for BcrR function in its native environment [3, 4].

#### 341 **DNA-binding activity of BcrR mutants R11K, S33L, G64D, E179K and T183M**

342 Previous investigations have found that BcrR requires membrane localisation for DNA-  
343 binding activity and function [4, 5]. Five BcrR mutants, R11K, S33L (from the DBD),  
344 G64D (oligomerisation domain), and E179K and T183M (localised to the second  
345 extracellular loop cluster of the TMD), were chosen for further functional  
346 characterisation. To determine whether these mutations influenced the DNA-binding  
347 capability of BcrR, EMSAs were performed with the *bcrABD* target promoter region  
348 ( $P_{bcrA}$ ) (Fig. 6a). A shift of the  $P_{bcrA}$  DNA probe was observed for WT BcrR and all five  
349 BcrR mutants (Fig. 6 b – g). No shift was observed in the absence of BcrR (Fig. 6h,  
350 liposome-only control). However, auto-fluorescence of the liposomes was detected.  
351 To avoid introduction of experimental artefact, densitometric analyses were  
352 subsequently performed on the probe (Fig. 6b – g and Fig. S5). The densitometric  
353 data shows that upon addition of BcrR-containing proteoliposomes, the relative band  
354 intensity of the probe decreases (Fig. S5). In the BcrR WT and S33L mutant, this shift  
355 is concentration-dependent (Fig. S5). For the BcrR R11K, G64D, E179K, and T183M  
356 mutants, a complete band shift is observed at the lowest ratio of BcrR:DNA (25:1) (Fig.  
357 S5). A non-labelled competitor probe (of the same length and nucleotide sequence as  
358  $^{\text{IRDye700}}P_{bcrA}$ ) was able to displace the labelled  $P_{bcrA}$  target probe at increasing  
359 concentrations, shown as an increase in free labelled probe and a decrease in bound  
360 probe (Fig. S6a, lanes 1 – 5). This additional control, alongside previous work that has



361 shown BcrR proteoliposomes bind a site-specific probe [4, 5], confirms BcrR WT and  
362 all five BcrR mutants are able to specifically bind the target *bcrA* DNA probe.

### 363 **Molecular modelling of the BcrR DNA-binding domain and theoretical analysis** 364 **of the DNA-binding domain mutants**

365 The DBD mutants R11K and S33L were able to recognise and bind to the *bcrABD*  
366 promoter, despite conferring a loss of BcrR function. Therefore, in order to further  
367 understand the implications of the R11K and S33L substitutions on BcrR function, a  
368 three-dimensional model of the DBD was constructed. A NCBI protein BLAST of the  
369 DBD (residues 1 - 69) against the Protein Databank identified the P22 c2 phage  
370 repressor DNA-binding domain (PDB sequence file: 3JXB), meeting the criteria of well-  
371 characterised and highest sequence homology (34%) (Fig. 7a). The P22 c2 phage  
372 repressor protein structure was used as a model in ProtMod for the structural analysis  
373 of the BcrR DNA-binding domain (Fig. 7b - d) [16]. The three-dimensional model  
374 predicts that five  $\alpha$  helices make up the BcrR DBD (helices 1 - 4), with helices 2 (16 -  
375 25) and 3 (28 - 37) forming the HTH motif, and bordering helices 1 (3 - 13) and 4 (44  
376 - 53) providing structural support (Fig. 7a and 7b). It also suggests BcrR forms a  
377 homodimer at each set of inverted repeats and highlights a potential dimerisation  
378 interface between residues 40 - 61 (helix 4 and 5) (Fig. 7b). This observation  
379 hypothesises functional overlap between the DBD and OGD, and therefore indicates  
380 oligomeric status could play an important role in transitioning the DBD from an  
381 inactivated to activated conformational state in the presence of bacitracin.

382 Virtual amino acid substitutions were carried out on the three-dimensional model for  
383 R11K and S33L using PyMOL (The PyMOL Molecular Graphics System, Version 1.7  
384 Schrödinger, LLC) (Fig. 7). An R11K substitution appears to disrupt a conserved salt

385 bridge between R11 (R14 in model) and E36 (E39) and eliminate the hydrogen bond  
386 between R11 and L16 (I19 in model) in the DBD model (Fig. 7c and d). The R11  
387 residue is conserved among XRE-type HTH DNA-binding domains (R14 in P22 c2 and  
388 R10 in 434) (Fig. 7a), and previous investigations in the P22 c2 and 434 Cro repressor  
389 have shown that this residue provides structural support to the HTH motif (helices 2  
390 and 3) through the observed salt bridge (R11 - E36) and hydrogen bond (R11 - L16)  
391 (Fig. 7c) [18, 19]. Disrupting this interaction in the 434 phage repressor (R10M)  
392 loosens the core structure of the DNA-binding domain and alters the DNA-binding  
393 surface of the protein [20]. We therefore hypothesise that a less dramatic R to K  
394 change at position 11 allows the BcrR R11K mutant to retain its ability to bind to the  
395 *bcrABD* target promoter as observed in the EMSA (Fig. 7c); but propose, loss of the  
396 hydrogen bond between R11 and L16 and weakening of the R11 - E36 salt bridge may  
397 alter the DNA-binding surface upon activation by bacitracin, thereby affecting the  
398 ability of BcrR R11K to induce transcription of the *bcrABD* operon.

399 The three-dimensional model predicts a S33L (S36 in model) substitution disrupts the  
400 direct hydrogen bond with the DNA phosphate oxygen due to the lack of a polar  
401 hydroxyl side group (Fig. 7c and d), which would suggest the loss of function in the  
402 S33L is likely due to inability to bind to the target promoter. However, the EMSAs show  
403 S33L retains its ability to bind and recognise the target promoter (Fig. 6d). We  
404 therefore hypothesise that some interactions at the protein and DNA interface are  
405 essential for constitutive binding to the DNA promoter, while others are essential for  
406 transducing bacitracin-dependent activation to the DNA promoter to allow initiation of  
407 transcription of *bcrABD* by RNA polymerase (RNAP).

408 The mechanism of promoter activation by BcrR is unknown, however it is thought that  
409 upon binding of bacitracin BcrR undergoes a conformational change. This is thought

410 to result in either a topological change in the *bcrABD* promoter exposing the core  
411 promoter elements to RNAP, or in recruitment of RNAP by the promoter-proximal  
412 dimer of BcrR [5]. Low-affinity protein-DNA operator complexes have previously been  
413 shown to reduce DNA-twisting [18, 21] therefore, it is conceivable that in the absence  
414 of either the R11 - L16 hydrogen bond, or the S33 - DNA hydrogen bond, BcrR is  
415 unable to transduce the signal from the bacitracin-binding site to the target promoter  
416 to allow exposure of the core promoter elements, and initiation of *bcrABD* expression.

### 417 **BcrR localisation to the cell membrane**

418 Membrane localisation is essential for BcrR function and therefore mutations in the  
419 transmembrane domain that confer a LOF likely result in a misfolded protein that is  
420 either displaced from the membrane, subjected to degradation, or insensitive to  
421 bacitracin. Two transmembrane domain mutants E179K and T183M were tested for  
422 cellular localisation, using BcrR WT and three mutants R11K, S33L, and G64D as  
423 controls. For these experiments, BcrR WT and mutants were expressed in *E. coli* as  
424 we have previously shown that functional BcrR localises to the membrane in this  
425 bacterium [4] and non-functional BcrR (membrane domain removed) localises to the  
426 cytoplasm [5]. Upon expression of BcrR WT and variants in *E. coli* cellular proteins  
427 were subsequently separated into membrane and cytosolic fractions. Fractions were  
428 analysed by SDS-PAGE and BcrR localisation probed by Western Blot (Fig. 8a and  
429 b). When the membrane fractions were run alongside the cytosolic (supernatant after  
430 ultracentrifugation) fraction, BcrR was clearly observed in the membrane fraction, and  
431 not in the cytosolic fraction (Fig. 8a). BcrR was found in the membrane fraction in all  
432 cases, confirming that membrane localisation does not play a role in either of the loss  
433 or gain of function BcrR mutants.

434 BcrR is reported to directly detect bacitracin, but the bacitracin-binding site of BcrR  
435 has not been identified [5]. Transmembrane receptor proteins such as sensor kinases  
436 ApsS and PhoQ, which regulate resistance to cationic antimicrobial peptides  
437 (CAMPs), are known to detect target ligands through their extracellular domains [22–  
438 24]. These proteins sense CAMPs at the membrane surface through an acidic  
439 extracellular loop that can vary in length from nine amino acids in ApsS to 145 in PhoQ,  
440 and while bacitracin is not a CAMP, it does have amphipathic properties [24, 25]. BcrR  
441 has two putative extracellular loops embedded in its C-terminal transmembrane  
442 domain. Seven LOF mutations were isolated in the TMD, with three (E179K, P180S,  
443 and T183M) clustered to the second extracellular loop. We have previously shown  
444 direct bacitracin-binding using tryptophan fluorescence, however this technique lacked  
445 the sensitivity to detect differences between WT and these LOF mutants (data not  
446 shown). Nevertheless, we hypothesise the second extracellular loop of the  
447 transmembrane domain may serve as a potential bacitracin-binding site, exploiting the  
448 hydrophilic and hydrophobic properties of this region to aid in binding of the  
449 amphipathic bacitracin.

450 AgrC binds its target peptide through a two-step process which involves initial non-  
451 specific interactions in the hydrophobic pocket formed by the transmembrane helices,  
452 followed by specific hydrophilic interactions provided by the final extracellular loop [26,  
453 27]. We hypothesise bacitracin binding may trigger conformational changes that are  
454 transduced to the DNA-binding domain, via the oligomerisation domain that activate  
455 BcrR. As the protein is constitutively bound to its target DNA, these conformational  
456 changes are then thought to change the local DNA topology and/or mediate direct  
457 interactions with RNAP [4, 5], leading to expression of *bcrABD* and ultimately  
458 activation of bacitracin resistance.

## 459 **Conclusion**

460 We originally identified the *bcr* locus in a bacitracin-resistant clinical isolate of *E.*  
461 *faecalis* using a transposon mutagenesis screen, which has since been identified in  
462 other Gram-positive bacteria, such as *Clostridium perfringens* [3, 28]. Acquired  
463 bacitracin resistance in *E. faecalis* is mediated by an ABC transporter (BcrAB) and a  
464 novel regulatory protein, BcrR [3]. Here, we have carried out random mutagenesis on  
465 the high-level bacitracin resistance regulator BcrR to further our understanding of how  
466 it functions as a membrane-bound one-component system. Fifteen unique point  
467 mutations were identified in *bcrR*, distributed across all three putative functional  
468 domains, the N-terminal XRE-type DNA-binding domain, intermediate oligomerisation  
469 domain, and C-terminal transmembrane domain. Of these fifteen mutations, fourteen  
470 conferred a loss of BcrR function, and one a hyper-sensitive GOF. Previous work has  
471 established *B. subtilis* and *E. coli* as heterologous hosts for analysis of BcrR function  
472 and we employed these systems here for further analysis of five BcrR mutants [4, 5,  
473 12]. Two mutants were identified at the G64 locus, a G64S substitution that  
474 significantly reduced bacitracin-induced BcrR activation and a G64D substitution that  
475 significantly increased activation compared to the WT. This G64D substitution also  
476 allowed BcrR activation in the absence of bacitracin under xylose-inducible  
477 expression. We propose a model that suggests the presence of glycine at position 64  
478 plays a critical role in regulating BcrR activation, thereby allowing expression of the  
479 resistance operon *bcrABD* only in the presence of bacitracin (Fig. S7). We hypothesise  
480 that this may also explain why even subtle substitutions such as G64S significantly  
481 alter BcrR activity (Fig 3b). Promoter activity assays were utilised to analyse  
482 transcription activation of the G64D gain of function mutant. They highlighted the  
483 importance of the oligomerisation domain- specifically G64 in regulating BcrR

484 activation in the presence of bacitracin (Fig. S7 and Fig. 9). We showed that the DNA-  
485 binding domain is not only important for binding the *bcrABD* promoter, but also for  
486 transducing and activating BcrR in the presence of bacitracin to allow initiation of  
487 *bcrABD* transcription by RNAP; and identified a potential bacitracin-binding site  
488 localised to a cluster of BcrR loss of function mutants at the second extracellular loop  
489 in the transmembrane domain (Fig. 9). BcrR was the first membrane-bound one-  
490 component high-level antimicrobial resistance regulator identified in bacteria. This  
491 work builds on our previous work as it highlights the essentiality of each functional  
492 domain, and their co-operation, in order to articulate an effective response.

493

#### 494 **Acknowledgements**

495 We would like to thank Christoph von Ballmoos and Linda Naesvik Oejemyr for their  
496 expert advice, and Rob Fagerlund for his technical assistance. This work was  
497 supported by a University of Otago PhD Scholarship and Publishing Bursary (R.L.D.),  
498 the Todd Foundation of New Zealand Excellence Scholarship (R.L.D.), and the  
499 Deutsche Forschungsgemeinschaft (DFG; grant GE2164/3-1) (S.G.).

500 We declare no conflict of interest.

#### 501 **Abbreviations**

502 ABC ATP-binding cassette; DDM *n*-dodecyl- $\beta$ -D-maltoside, EMSA electrophoretic  
503 mobility shift assays; GOF gain of function; HA hydroxylamine hydrochloride; *lacZ*  $\beta$ -  
504 galactosidase; LB lysogeny broth; LOF loss of function; *luxABCDE* luciferase; MUG 4-  
505 methylumbelliferyl  $\beta$ -D-galactoside; NC negative control;  $P_{bcrA}$  *bcrA* promoter; WT wild-  
506 type.

507

508 **References**

- 509 1. **Ulrich LE, Koonin E V, Zhulin IB.** One-component systems dominate signal  
510 transduction in prokaryotes. *Trends Microbiol* 2005;13:52–56.
- 511 2. **Cuthbertson L, Nodwell JR.** The TetR family of regulators. *Microbiol Mol Biol*  
512 *Rev* 2013;77:440–475.
- 513 3. **Manson JM, Keis S, Smith JMB, Cook GM.** Acquired bacitracin resistance in  
514 *Enterococcus faecalis* is mediated by an ABC transporter and a novel  
515 regulatory protein, BcrR. *Antimicrob Agents Chemother* 2004;48:3743–3748.
- 516 4. **Gauntlett JC, Gebhard S, Keis S, Manson JM, Pos KM, et al.** Molecular  
517 analysis of BcrR, a membrane-bound bacitracin sensor and DNA-binding  
518 protein from *Enterococcus faecalis*. *J Biol Chem* 2008;283:8591–8600.
- 519 5. **Gebhard S, Gaballa A, Helmann JD, Cook GM.** Direct stimulus perception  
520 and transcription activation by a membrane-bound DNA binding protein. *Mol*  
521 *Microbiol* 2009;73:482–491.
- 522 6. **Dintner S, Heermann R, Fang C, Jung K, Gebhard S.** A sensory complex  
523 consisting of an ATP-binding-cassette transporter and a two-component  
524 regulatory system controls bacitracin resistance in *Bacillus subtilis*. *J Biol*  
525 *Chem* 2014;289:27899–27910.
- 526 7. **Gebhard S, Fang C, Shaaly A, Leslie DJ, Weimar MR, et al.** Identification  
527 and characterization of a bacitracin resistance network in *Enterococcus*  
528 *faecalis*. *Antimicrob Agents Chemother* 2014;58:1425–1433.
- 529 8. **Ohki R, Giyanto, Tateno K, Masuyama W, Moriya S, et al.** The BceRS two-

- 530 component regulatory system induces expression of the bacitracin transporter,  
531 BceAB, in *Bacillus subtilis*. *Mol Microbiol* 2003;49:1135–1144.
- 532 9. **Bernard R, Guiseppi A, Chippaux M, Foglino M, Denizot F.** Resistance to  
533 bacitracin in *Bacillus subtilis*: Unexpected requirement of the BceAB ABC  
534 transporter in the control of expression of its own structural genes. *J Bacteriol*  
535 2007;189:8636–8642.
- 536 10. **Rietkötter E, Hoyer D, Mascher T.** Bacitracin sensing in *Bacillus subtilis*. *Mol*  
537 *Microbiol* 2008;68:768–785.
- 538 11. **Harwood S, Cutting C (eds).** *Molecular Biological methods for Bacillus*.  
539 Chichester, England: John Wiley & Sons, Inc.; 1990.
- 540 12. **Fang C, Stiegeler E, Cook GM, Mascher T, Gebhard S.** *Bacillus subtilis* as a  
541 platform for molecular characterisation of regulatory mechanisms of  
542 *Enterococcus faecalis* resistance against cell wall antibiotics. *PLoS One*  
543 2014;9:1–10.
- 544 13. **Patterson AG, Chang JT, Taylor C, Fineran PC.** Regulation of the Type I-F  
545 CRISPR-Cas system by CRP-cAMP and GalM controls spacer acquisition and  
546 interference. *Nucleic Acids Res* 2015;43:6038–6048.
- 547 14. **Ho SN, Hunt HD, Horton RM, Pullen JK, Pease LR.** Site-directed  
548 mutagenesis by overlap extension using the polymerase chain reaction. *Gene*  
549 1989;77:51–59.
- 550 15. **Nesterenko M V., Tilley M, Upton SJ.** A simple modification of Blum’s silver  
551 stain method allows for 30 minute detection of proteins in polyacrylamide gels.  
552 *J Biochem Biophys Methods* 1994;28:239–242.



- 553 16. **Webb B, Sali A.** Comparative protein structure modeling using MODELLER.  
554 *Curr Protoc Bioinformatics* 2014;47:1–32.
- 555 17. **Radeck J, Kraft K, Bartels J, Cikovic T, Dürr F, et al.** The Bacillus BioBrick  
556 Box: generation and evaluation of essential genetic building blocks for  
557 standardized work with *Bacillus subtilis*. *J Biol Eng* 2013;7:29.
- 558 18. **Mondragón A, Subbiah S, Almo SC, Drottar M, Harrison SC.** Structure of  
559 the amino-terminal domain of phage 434 repressor at 2.0 Å resolution. *J Mol*  
560 *Biol* 1989;205:189–200.
- 561 19. **Sevilla-Sierra P, Otting G, Wüthrich K.** Determination of the nuclear  
562 magnetic resonance structure of the DNA-binding domain of the P22 c2  
563 repressor (1 to 76) in solution and comparison with the DNA-binding domain of  
564 the 434 repressor. *J Mol Biol* 1994;235:1003–1020.
- 565 20. **Pervushin K, Billeter M, Siegal G, Wüthrich K.** Structural role of a buried  
566 salt bridge in the 434 repressor DNA-binding domain. *J Mol Biol*  
567 1996;264:1002–1012.
- 568 21. **Harrison SC, Aggarwal AK.** DNA recognition by proteins with the helix-turn-  
569 helix motif. *Annu Rev Biochem* 1990;59:933–969.
- 570 22. **Bader MW, Sanowar S, Daley ME, Schneider AR, Cho U, et al.** Recognition  
571 of antimicrobial peptides by a bacterial sensor kinase. *Cell* 2005;122:461–472.
- 572 23. **Li M, Lai Y, Villaruz AE, Cha DJ, Sturdevant DE, et al.** Gram-positive three-  
573 component antimicrobial peptide-sensing system. *Proc Natl Acad Sci U S A*  
574 2007;104:9469–74.
- 575 24. **Otto M.** Bacterial sensing of antimicrobial peptides. *Contrib Microbiol*

576 2009;16:136–149.

577 25. **Economou NJ, Cocklin S, Loll PJ.** High-resolution crystal structure reveals  
578 molecular details of target recognition by bacitracin. *Proc Natl Acad Sci U S A*  
579 2013;110:14207–12.

580 26. **Lyon GJ, Novick RP.** Peptide signaling in *Staphylococcus aureus* and other  
581 Gram-positive bacteria. *Peptides* 2004;25:1389–1403.

582 27. **Mascher T, Helmann JD, Uden G.** Stimulus perception in bacterial signal-  
583 transducing histidine kinases. *Microbiol Mol Biol Rev* 2006;70:910–938.

584 28. **Charlebois A, Jalbert LA, Harel J, Masson L, Archambault M.**  
585 Characterization of genes encoding for acquired bacitracin resistance in  
586 *Clostridium perfringens*. *PLoS One* 2012;7:e44449.

587

588

589

590

591

592

593

594

595

596

597

598 **Table 1. Identification of BcrR loss and gain of function point mutations**

<b>Mutant No.</b>	<b>Domain</b>	<b>Base No.</b>	<b>Base change</b>	<b>AA change</b>	<b>Colour</b>	<b>Status</b>	<b>Frequency‡</b>
BcrR8	DBD*	31	G-A	R11K	White	OFF	2
BcrR7	"	49	C-T	T17M	White	OFF	1
BcrR31	"	88	C-T	T30I	White	OFF	1
BcrR39	"	98	C-T	S33L	White	OFF	1
BcrR30	OGD#	124	C-T	P42L	White	OFF	3
BcrR17	"	151	C-T	S51F	White Blue/	OFF	3
BcrR21	"	189	G-A	G64S	White	OFF	1
BcrR37	"	190	G-A	G64D	Blue	ON	2
BcrR10	TMD†	261	G-A	G88R	White	OFF	2
BcrR28	"	301	C-T	P101L	White Blue/	OFF	1
BcrR18	"	367	C-T	T123I	White	OFF	1
BcrR1	"	421	G-A	G141D	White	OFF	1
BcrR16	"	534	G-A	E179K	White Blue/	OFF	2
BcrR11	"	537	C-T	P180S	White	OFF	1
BcrR14	"	547	C-T	T183M	White	OFF	3

599

600 \*DBD DNA-binding domain; #OGD oligomerisation domain; †transmembrane domain;

601 ‡the number of times a point mutation was isolated.

602

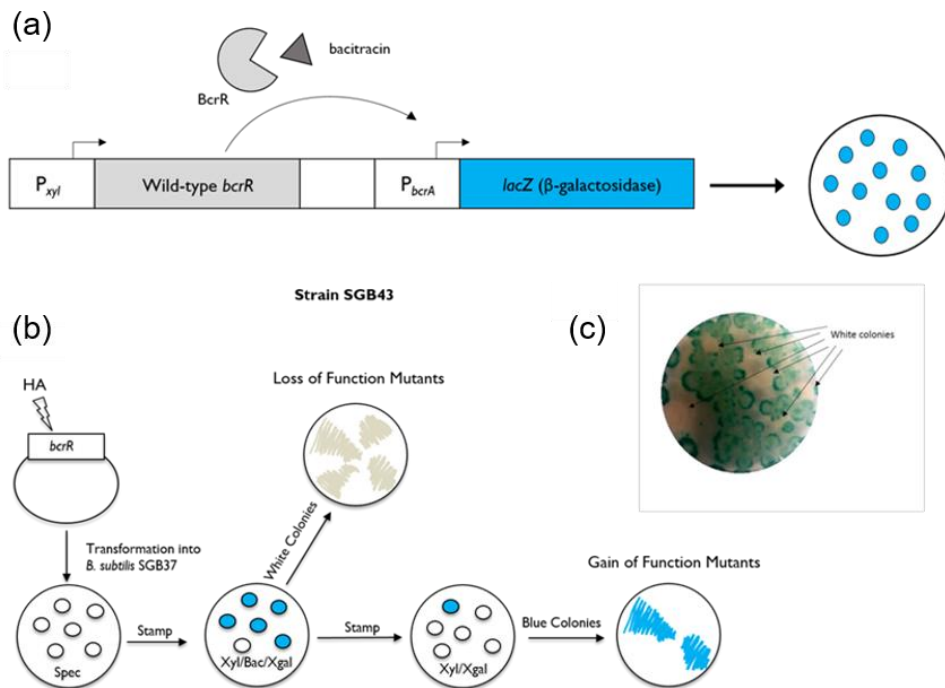
603

604

605

606

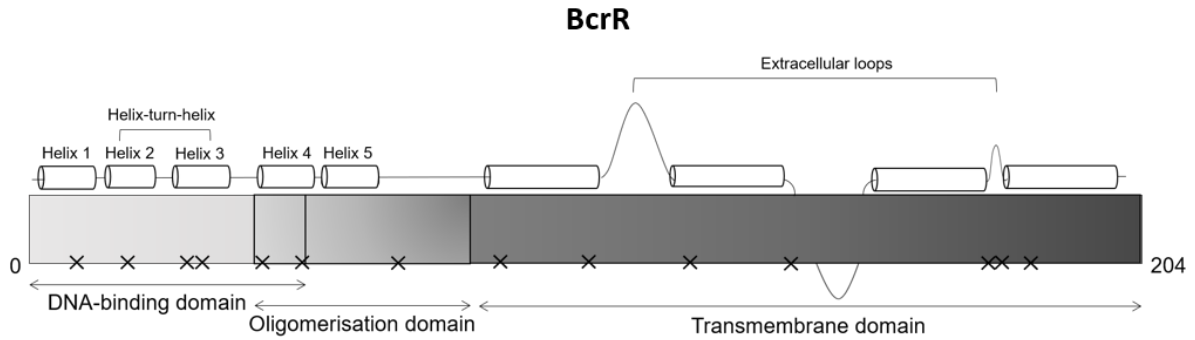
607



608

609 **Fig. 1. Identification of *bcrR* mutants using a  $\beta$ -galactosidase reporter ( $P_{bcrA}$ -**  
 610 ***lacZ*).** Wild-type (WT) *bcrR* was cloned into the plasmid pXT under the xylose-  
 611 inducible promoter to form pXT-*bcrR*. The *B. subtilis* strain SGB37 was transformed  
 612 with pXT-*bcrR*, integrating upstream of the  $\beta$ -galactosidase reporter ( $P_{bcrA}$ -*lacZ*), to  
 613 form the positive control strain SGB43 (a). In the positive control, WT BcrR is  
 614 expressed and activated upon the addition of xylose (Xyl; 0.2%) and bacitracin (Bac;  
 615 0.5  $\mu\text{g ml}^{-1}$ ) respectively. Activated WT BcrR subsequently binds the  $P_{bcrA}$  promoter  
 616 inducing expression of the  $\beta$ -galactosidase reporter, thereby producing blue colonies  
 617 on LB agar plates containing Xgal (100  $\mu\text{g ml}^{-1}$ ) (a). In a separate experiment, pXT-  
 618 BcrR plasmid DNA was mutagenised with hydroxylamine hydrochloride (HA),  
 619 purified, and transformed into SGB37 (b). Transformants were plated on LB  
 620 spectinomycin (spec) selection agar and the resulting colonies were subsequently  
 621 stamped onto LB agar plates containing a combination of Xyl, Xgal, and Bac. This was  
 622 used to screen for BcrR loss of function (LOF) and gain of function (GOF) mutants  
 623 using a modified blue/white protocol [12]. In the presence of WT or GOF BcrR colonies  
 624 were blue, while BcrR LOF mutants were white (b). Colonies from Xyl/Bac/Xgal plates  
 625 were stamped on Xyl/Xgal only plates to select for blue GOF mutants (b and c).

626



627

628 **Fig. 2. Mapping of LOF and GOF mutations on the BcrR protein.** BcrR is a 204  
 629 amino acid protein that consists of three putative functional domains: a N-terminal  
 630 DNA-binding domain (light grey), an oligomerisation domain (medium grey), and a C-  
 631 terminal transmembrane domain (dark grey). Loss and gain of function mutations (X)  
 632 were mapped to the BcrR protein sequence to visualise the distribution of mutations.

633

634

635

636

637

638

639

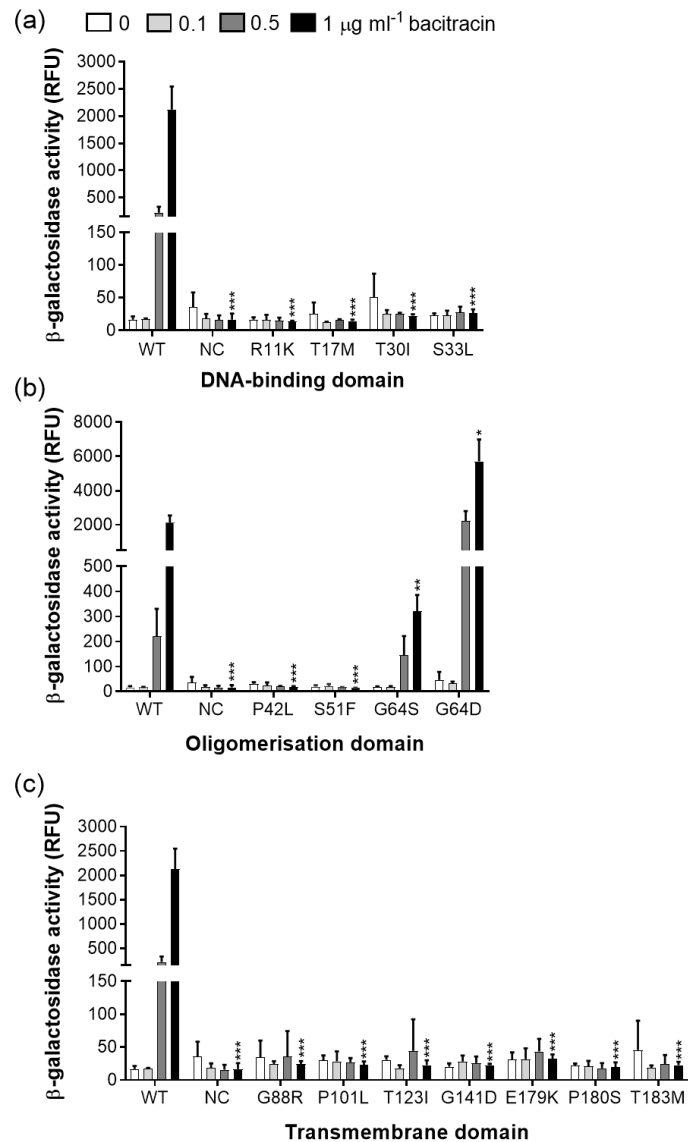
640

641

642

643

644

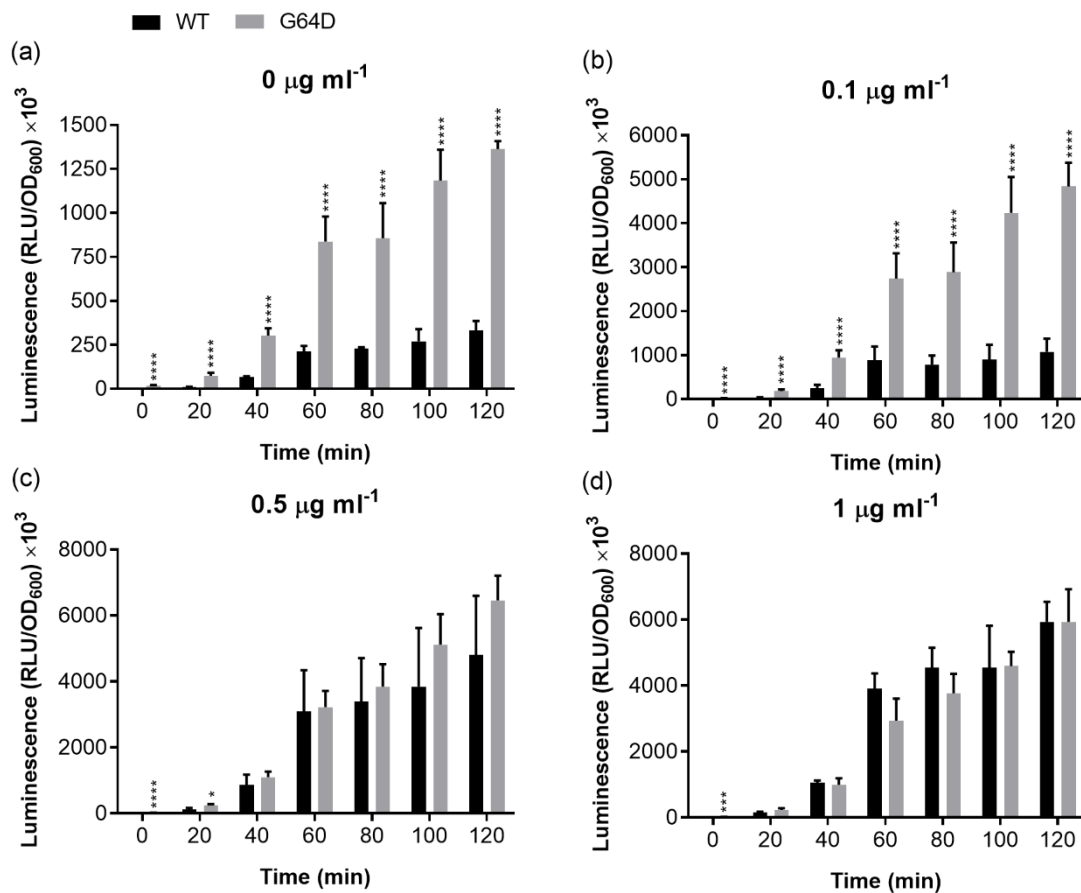


645

646 **Fig. 3. BcrR activity in response to bacitracin using a  $P_{bcrA}$ -lacZ reporter.**

647 Expression of the integrative  $P_{bcrA}$ -lacZ promoter under the control of wild-type (WT)  
 648 and mutant BcrR was measured using  $\beta$ -galactosidase activity. BcrR mutant activity  
 649 is presented alongside WT and an empty vector negative control (NC) with data  
 650 separated into putative functional domains: the DNA-binding domain (a),  
 651 oligomerisation domain (b), and transmembrane domain (c). Data shown are the mean  
 652  $\pm$ SD ( $n$  = biological triplicate). Statistical significance was determined by performing  
 653 an unpaired  $t$ -test of BcrR variants relative to WT at a bacitracin concentration of 1  $\mu\text{g}$   
 654  $\text{ml}^{-1}$  ( $p$  values: (\*)  $< 0.05$ , (\*\*)  $< 0.01$ , (\*\*\*)  $< 0.005$ ).

655



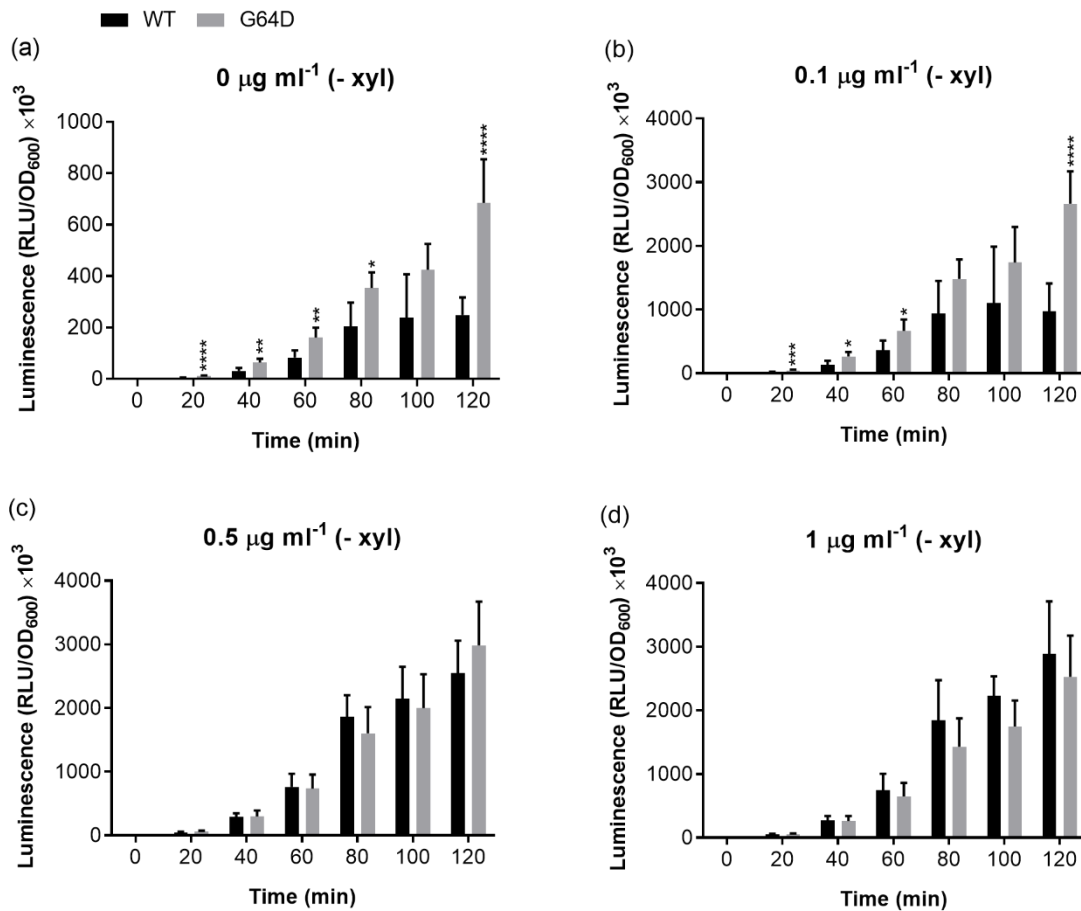
656

657 **Fig. 4. BcrR wild-type (WT) and G64D activity in response to bacitracin in the**  
 658 **presence of xylose using the  $P_{bcrA}$ -luxABCDE reporter.** BcrR expression is  
 659 controlled by a xylose-inducible promoter cloned upstream of the BcrR gene in the *B.*  
 660 *subtilis* heterologous host. BcrR WT and G64D mutant activity was monitored under  
 661 high (+ xylose) by measuring luciferase luminescence. WT and G64D BcrR activity  
 662 were compared at bacitracin concentrations of 0, 0.1, 0.5, and 1 µg ml<sup>-1</sup> over a period  
 663 of 120 min (a - d respectively). Data shown are the mean ± SD (*n* = biological  
 664 quadruplicate). Statistical significance was determined by performing an unpaired *t*-  
 665 test of G64D relative to WT (*p* values: (\*) <math>< 0.05</math>, (\*\*) <math>< 0.01</math>, (\*\*\*) <math>< 0.005</math>, (\*\*\*\*) <math>< 0.001</math>).

666

667

668



669

670 **Fig. 5. BcrR WT and G64D activity in response to bacitracin in the absence of**  
 671 **xylose using the *P<sub>bcrA</sub>-luxABCDE* reporter.** BcrR WT and G64D mutant activity was  
 672 monitored under low BcrR expression at bacitracin concentrations of 0, 0.1, 0.5 and 1  
 673 µg ml<sup>-1</sup> using a *P<sub>bcrA</sub>-luxABCDE* reporter (a – d). Activity was measured every 20 min  
 674 for 120 min. Data shown are the mean ±SD (*n* = biological quadruplicate). Statistical  
 675 significance was determined by performing an unpaired *t*-test of G64D relative to WT  
 676 (*p* values: (\*) <0.05, (\*\*) <0.01, (\*\*\*) <0.005, (\*\*\*\*) <0.001).

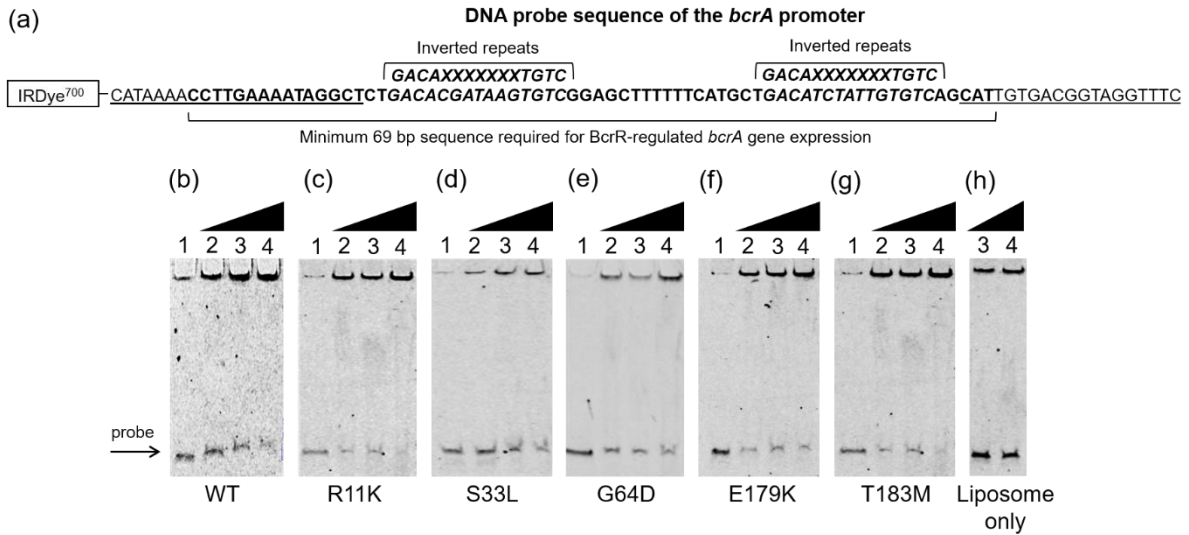
677

678

679

680





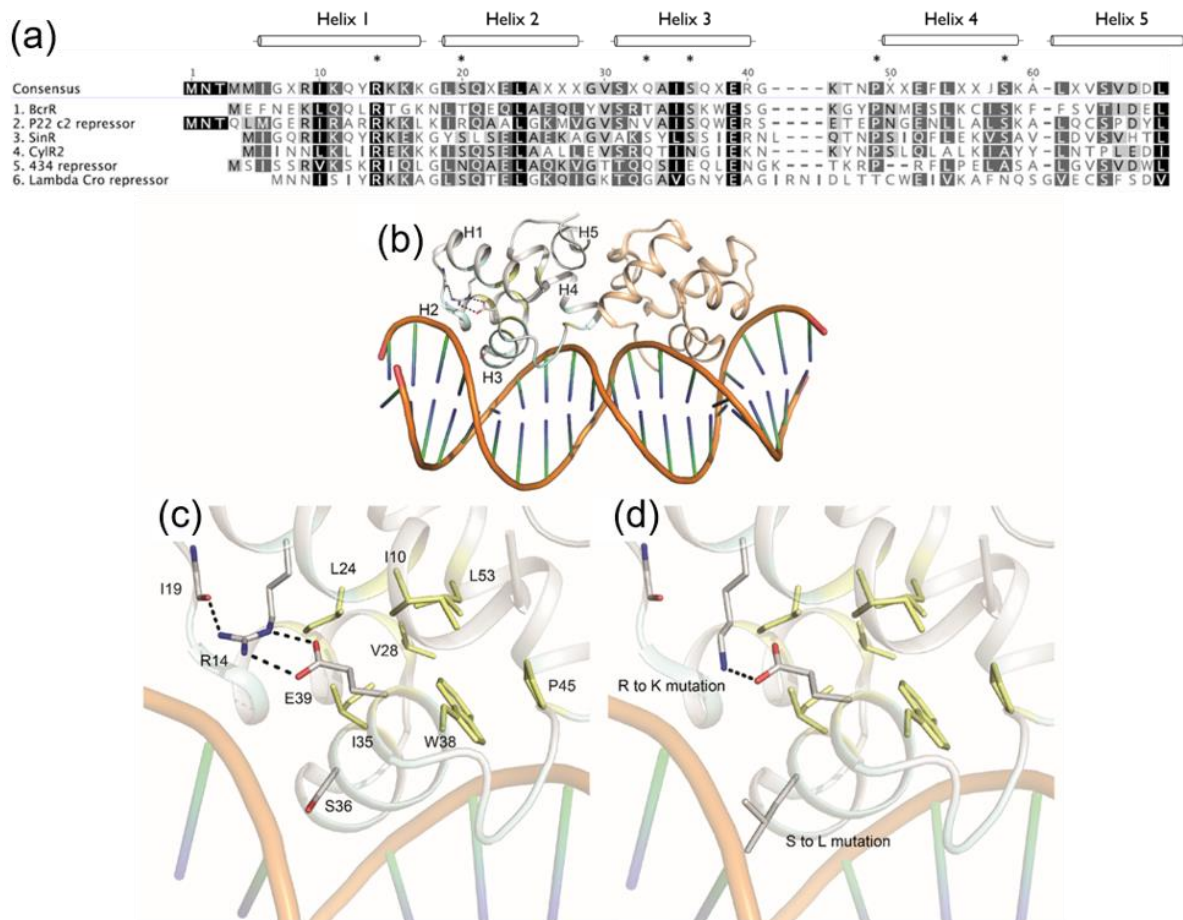
681

682 **Fig. 6. DNA-binding profiles of WT and mutant BcrR to  $P_{bcrA}$ .** (a) A 92 bp DNA  
 683 probe ( $P_{bcrA}$ ) was amplified from the *bcrA* promoter sequence and labelled with a 5'  
 684 fluorescent IRDye<sup>700</sup> tag for visualisation. This probe contained the 69 bp sequence  
 685 (bold) necessary for *bcrA* expression, including the set of inverted repeats (bold and  
 686 italicised) that are essential for BcrR DNA-binding [4,5]. The DNA-binding profiles of  
 687 BcrR wild-type (WT) (b) and five BcrR mutants R11K (c), S33L (d), G64D (e), E179K  
 688 (f), T183M (g) to the *bcrA* target promoter were compared using electrophoretic  
 689 mobility shift assays.  $P_{bcrA}$  was incubated with BcrR WT and mutant proteoliposomes  
 690 at protein: DNA molar ratios of 0:1 (lane 1), 25:1 (lane 2), 50:1 (lane 3), 125:1 (lane 4)  
 691 the probe concentration.  $P_{bcrA}$  was shifted in a BcrR concentration-dependent manner  
 692 in BcrR WT and all five mutants; no shift was observed in the absence of BcrR (lane  
 693 1) and no concentration-dependent shift was observed in the liposome only control  
 694 (h). Lipid concentrations in lane 3 and 4 (h) are relative to lane 3 and 4 (b – g). Binding  
 695 reactions were run on a 6% native PAGE gel at 350V for 25 min and visualised at 700  
 696 nm. The gels presented here are a representative of shifts that have been repeated at  
 697 least three times.

698

699

700



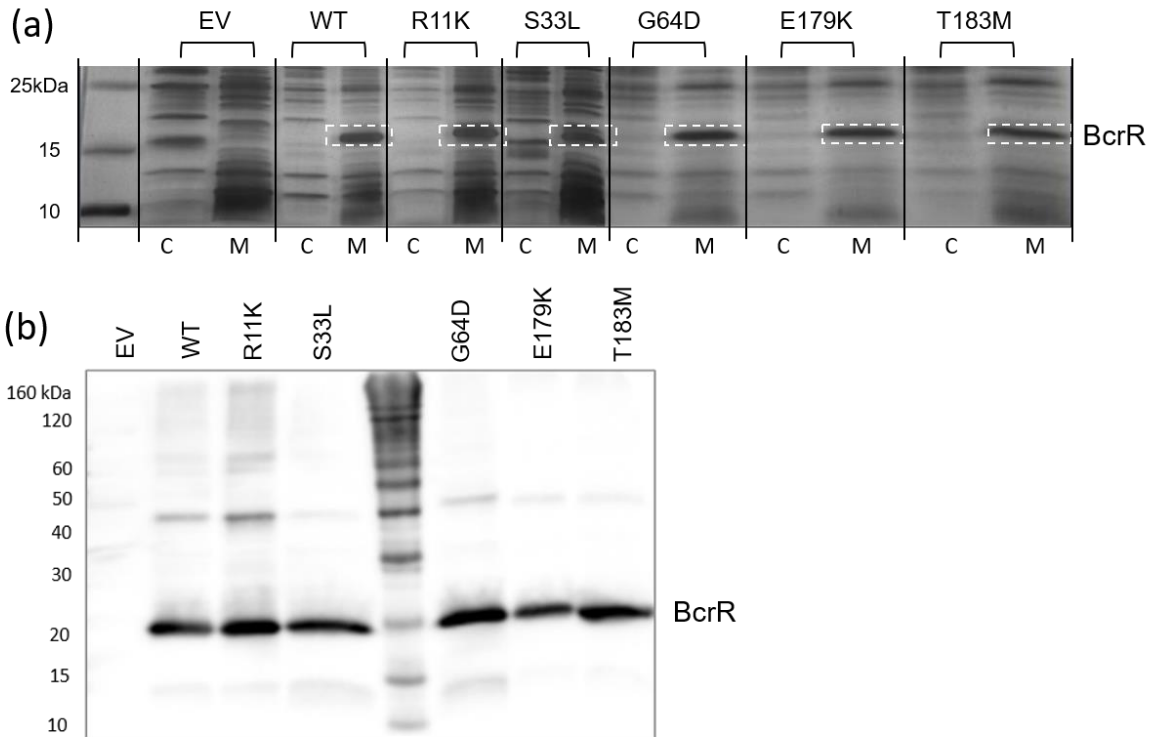
701

702 **Fig. 7. A three-dimensional model of the BcrR DNA-binding domain.** The BcrR  
 703 DNA-binding domain sequence was aligned with five well-characterised XRE-type  
 704 HTH DNA-binding proteins (a). The P22 c2 phage repressor protein had the highest  
 705 sequence homology with the BcrR DNA-binding domain. The P22 c2 structure was  
 706 used as a model in ProtMod for the structural analysis of the BcrR DNA-binding  
 707 domain. The DNA-binding domain consists of five  $\alpha$  helices labelled 1-5 with helices 2  
 708 and 3 composing the HTH motif (b). Interactions between BcrR mutant residues, other  
 709 residues in the DNA-binding domain, and the target DNA promoter sequence were  
 710 analysed using PyMOL (c). DNA-binding domain wild-type (WT) residues were  
 711 substituted with their mutant counterparts to observe consequential changes to their  
 712 WT interactions (d - f).

713

714

715



716

717 **Fig. 8. Localisation of BcrR WT and mutants to the cell membrane.** Cell cytosolic  
 718 (C) and membrane (M) fractions of the empty vector control (EV), BcrR wild-type (WT),  
 719 and mutants R11K, S33L, G64D, E179K, and T183M from the protein localisation  
 720 experiment (about 200-500  $\mu$ g total protein) were run on a 12.5% SDS-PAGE gel  
 721 alongside a BenchMark™ His-tagged protein ladder (a). Membrane fractions were  
 722 rerun on a 12.5% SDS-PAGE gel for Western Blot analysis. BcrR WT and mutant  
 723 protein contained a His<sub>6</sub> C-terminal tag were subsequently probed for using an anti-  
 724 His antibody. BcrR was detected in all membrane fractions, except the negative control  
 725 (EV) (b).

726

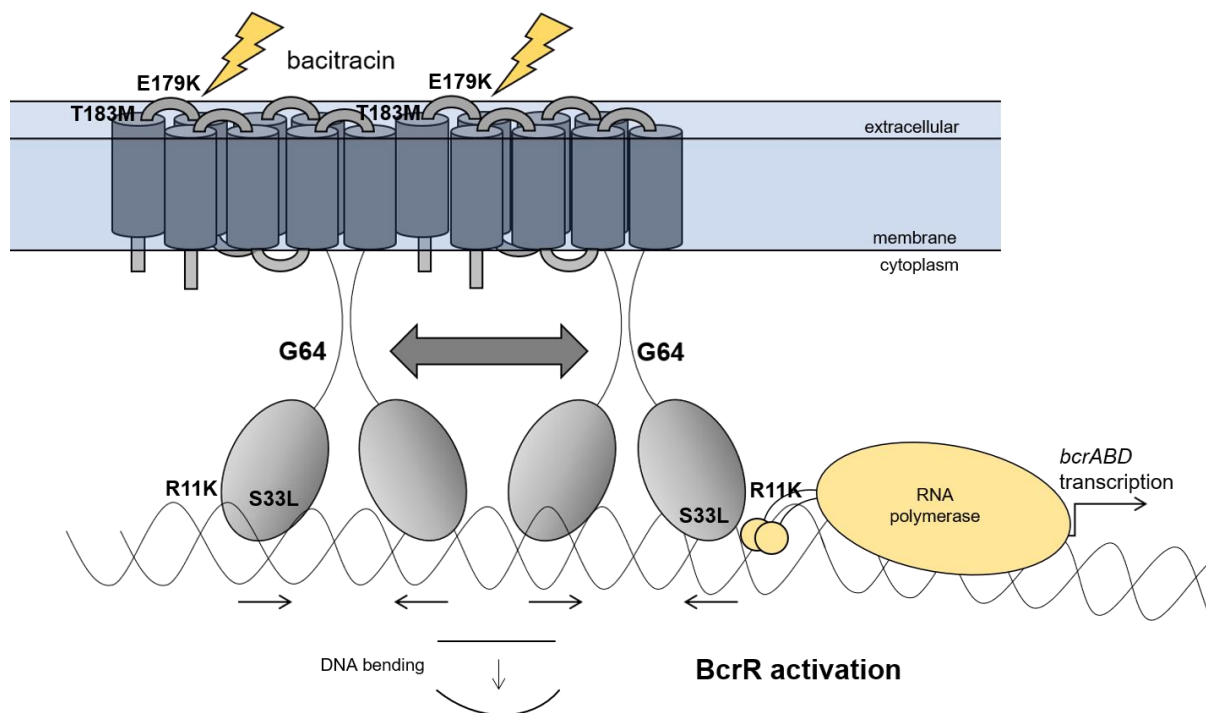
727

728

729

730

731



732

733 **Fig. 9. Schematic of bacitracin sensing and transcriptional activation by BcrR.**

734 BcrR directly senses bacitracin and elicits a response through activation and  
 735 subsequent initiation of *bcrABD* transcription. In this model BcrR detects bacitracin  
 736 through a putative bacitracin-binding site localised to the second extracellular loop of  
 737 the C-terminal transmembrane domain (E179K, P180S, and T183M). BcrR is  
 738 constitutively bound to the *bcrA* promoter ( $P_{bcrA}$ ) but requires bacitracin for activation,  
 739 likely through a conformational change, such as the oligomerisation of the BcrR dimers  
 740 to form an active BcrR tetramer. Glycine 64 (G64) likely plays an essential role in this  
 741 process. The BcrR DNA-binding domain contains five putative  $\alpha$  helices with a  
 742 conserved XRE-type helix-turn-helix DNA-binding motif. R11 and S33 appear to have  
 743 a crucial functional role in transducing the bacitracin activating signal to the DNA  
 744 promoter. We hypothesise R11 and S33 are required for bacitracin-dependent  
 745 changes in the local DNA topology, perhaps bending the DNA, to expose the binding  
 746 site for RNA polymerase, allowing transcription of the *bcrABD* operon.

747

748

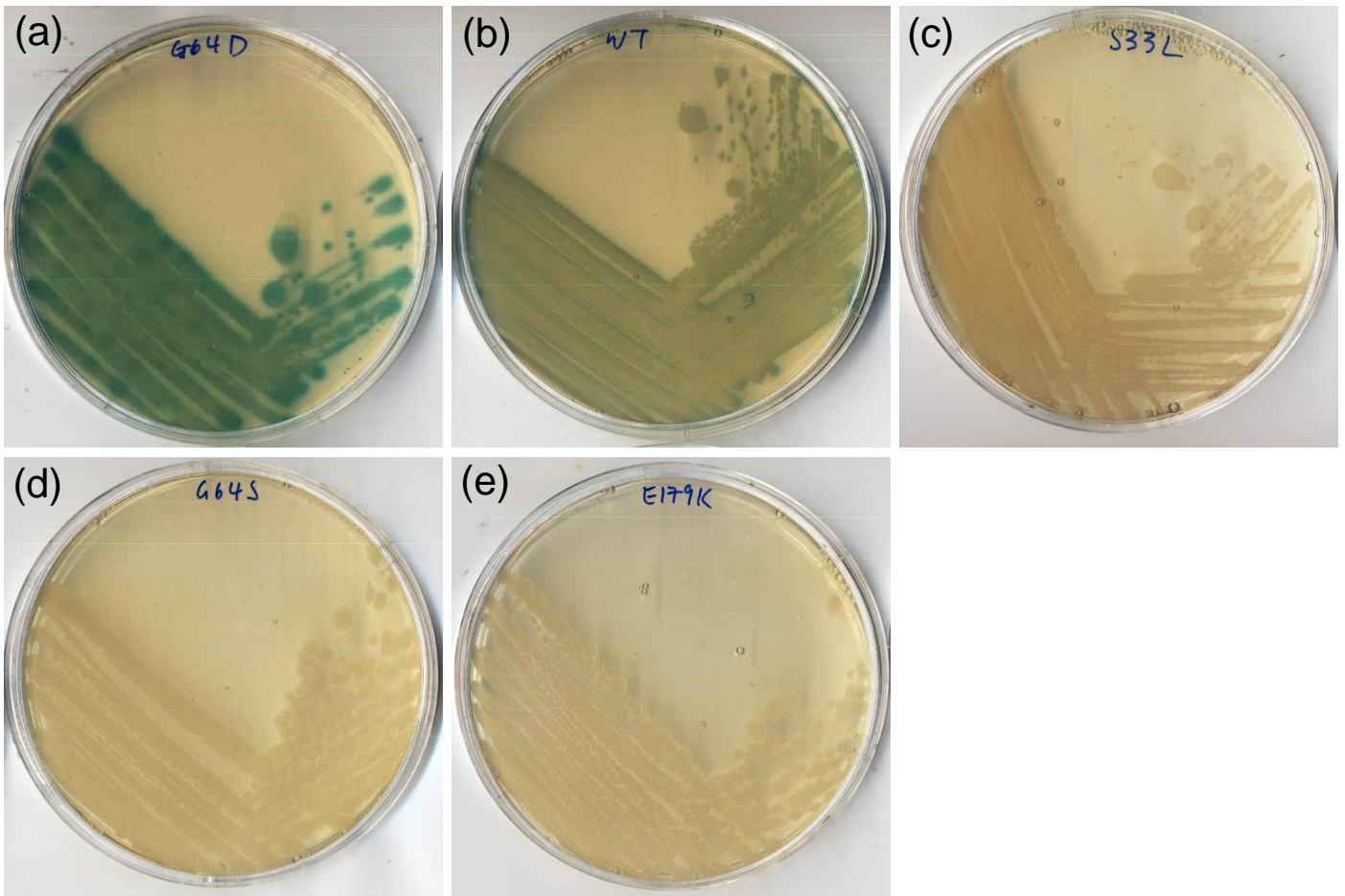


**Fig. S1. BcrR WT and mutant transformation into the  $P_{bcrA}$ -*lacZ* reporter strain *B. subtilis* SGB37.** Clonal cultures of the  $P_{bcrA}$ -*lacZ* reporter strain *B. subtilis* SGB37 were independently transformed with genomic DNA (gDNA) containing either the  $P_{xyI}$ -*bcrR* wild-type (WT) or mutant construct (S33L, G64S, G64D, and E179K). Transformants were plated on LB<sub>spec</sub> agar to select for gDNA containing the  $P_{xyI}$ -*bcrR* constructs. Three colonies were chosen for each *bcrR* variant and streaked onto LB<sub>xyI,bac,xgal</sub> agar and incubated at 37°C overnight. A representative photograph is presented here for each *bcrR* variant. The G64D gain of function mutant appears as blue colonies (a) which represents activated BcrR and are darker than the light blue WT colonies (b). The colonies of the loss of function mutants S33L (c), G64S (d), and E179K (e), appear white in colour, which represents a lack of active BcrR, i.e. loss of function.

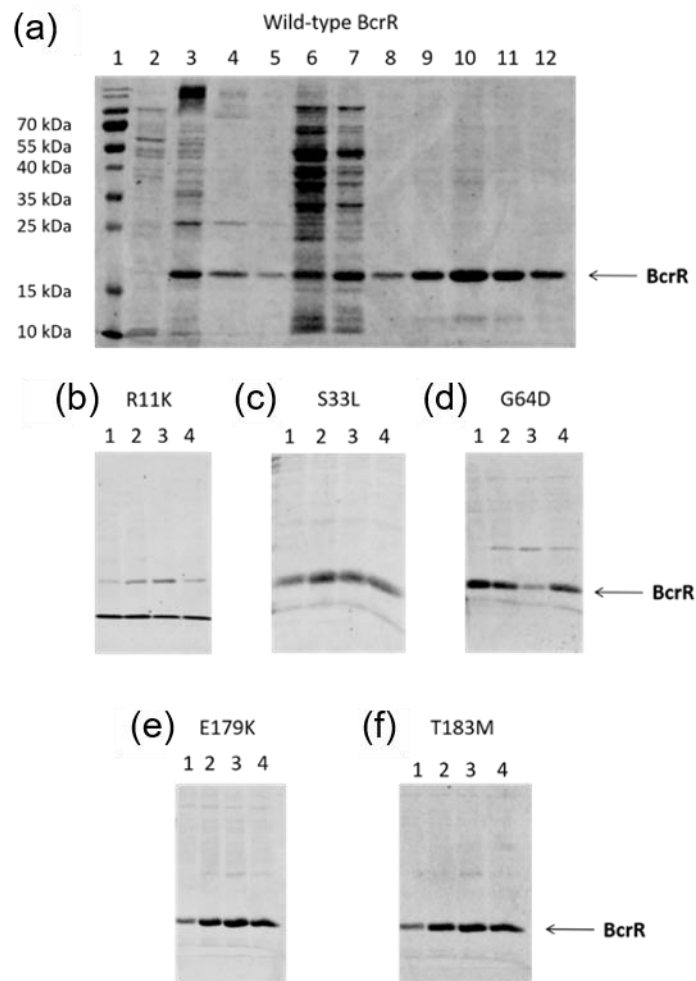


**Fig. S2. SDS-PAGE of purified wild-type (WT) and mutant BcrR protein.** BcrRHis protein was purified in a series of sequential steps. Samples were taken after each step and run on a 12.5% SDS-PAGE gel after purification. (a) Lane 2: supernatant from the sodium cholate wash to ensure BcrR was not removed from the membrane. Lanes 3,4,5: Sequential DDM solubilisation of BcrR. Lanes 6,7: protein fractions from the non-specifically bound protein. Lanes 8-12: protein fractions from the BcrR peak (these fractions were pooled for dialysis). (b - f) Lanes 1-3: purified BcrR fractions from the second purification peak for each of the BcrR mutants. Lane 4 (b - f): shows BcrR after fractions are pooled and dialysed. 10  $\mu$ l of sample were run regardless of total protein concentration (this equates to about 50  $\mu$ g in the purified protein lanes).

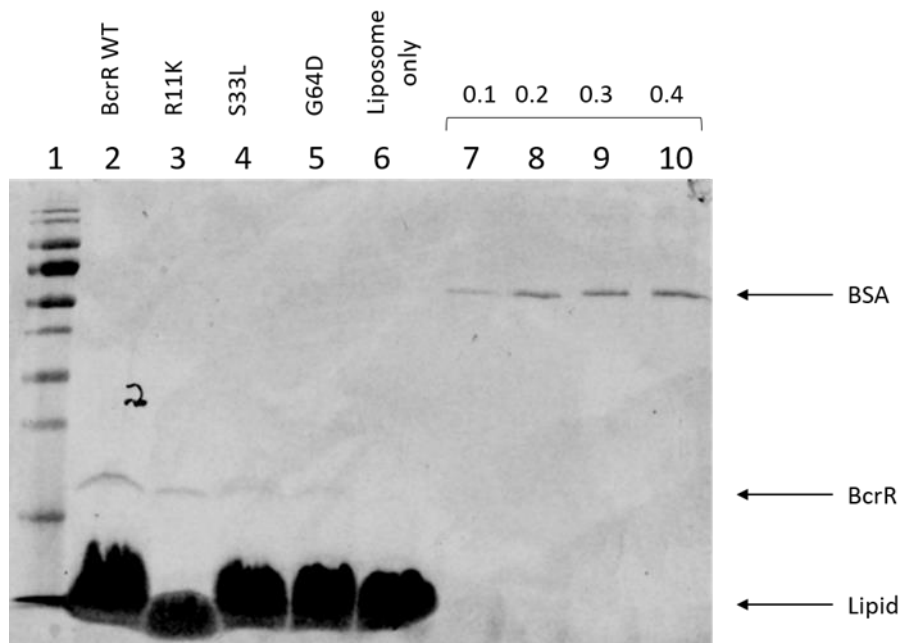


**Fig. S3. BcrR protein concentration in reconstituted liposomes by SDS-PAGE gel electrophoresis.** Wild-type (WT) BcrR protein and protein of BcrR mutants R11K, S33L, and G64D was purified and reconstituted into phosphatidyl choline liposomes. BcrR protein concentration in reconstituted proteoliposomes was determined by running 1.5  $\mu\text{l}$  of BcrR WT (2), R11K (3), S33L (4), and G64D (5) proteoliposome on a 4  $\times$  SDS-concentrated 12.5% SDS-PAGE gel against a BSA standard at a range of 0.1 - 0.4  $\text{mg ml}^{-1}$  (7 - 10). Protein size was determined by PageRuler™ protein ladder (1). A liposome only negative control was used to show absence of BcrR.

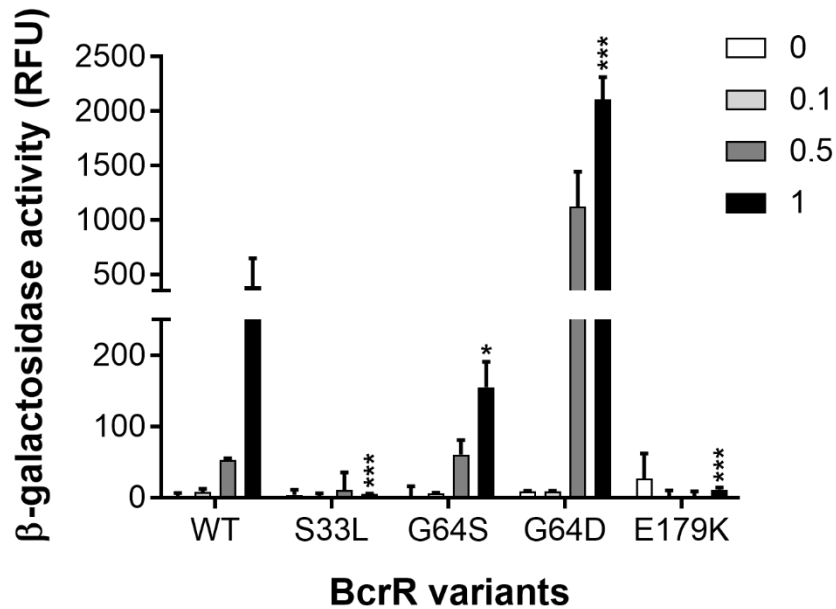


**Fig. S4. BcrR activity in response to bacitracin using a  $P_{bcrA}$ -*lacZ* reporter.** To confirm phenotypic observations of the new transformants, expression of the integrative  $P_{bcrA}$ -*lacZ* promoter under the control of wild-type (WT) and mutant BcrR was measured using  $\beta$ -galactosidase activity. BcrR mutant activity is presented alongside WT. Data shown are the mean  $\pm$ SD ( $n$  = biological triplicate). Statistical significance was determined by performing an unpaired  $t$ -test of BcrR variants relative to WT ( $p$  values: (\*)  $<0.05$ , (\*\*)  $<0.01$ , (\*\*\*)  $<0.005$ ).



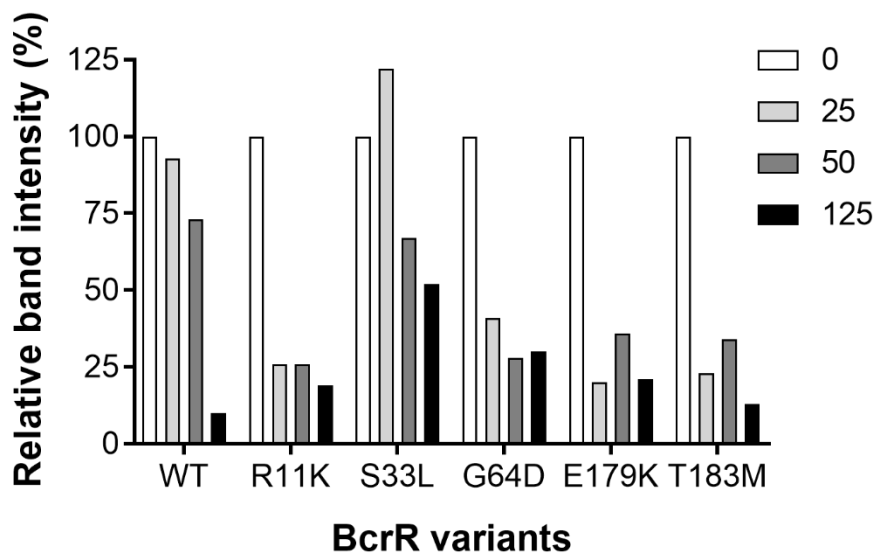


**Fig. S5. Densitometric analysis of the free probe in the electrophoretic mobility shift assays.** Band intensities are expressed relative (%) to the probe only band (Fig. 6. lane 1 (b – g)) in each electrophoretic mobility shift assay for each BcrR variant. White bars, no BcrR proteoliposomes (Fig. 6. lane 1 (b – g)), light grey bars protein:DNA molar ratio of 25:1 (Fig. 6. lane 2 (b – g)), dark grey bars 50:1 (Fig. 6. lane 3 (b – g)), and black bars 125:1 (Fig. 6. lane 4 (b – g)).

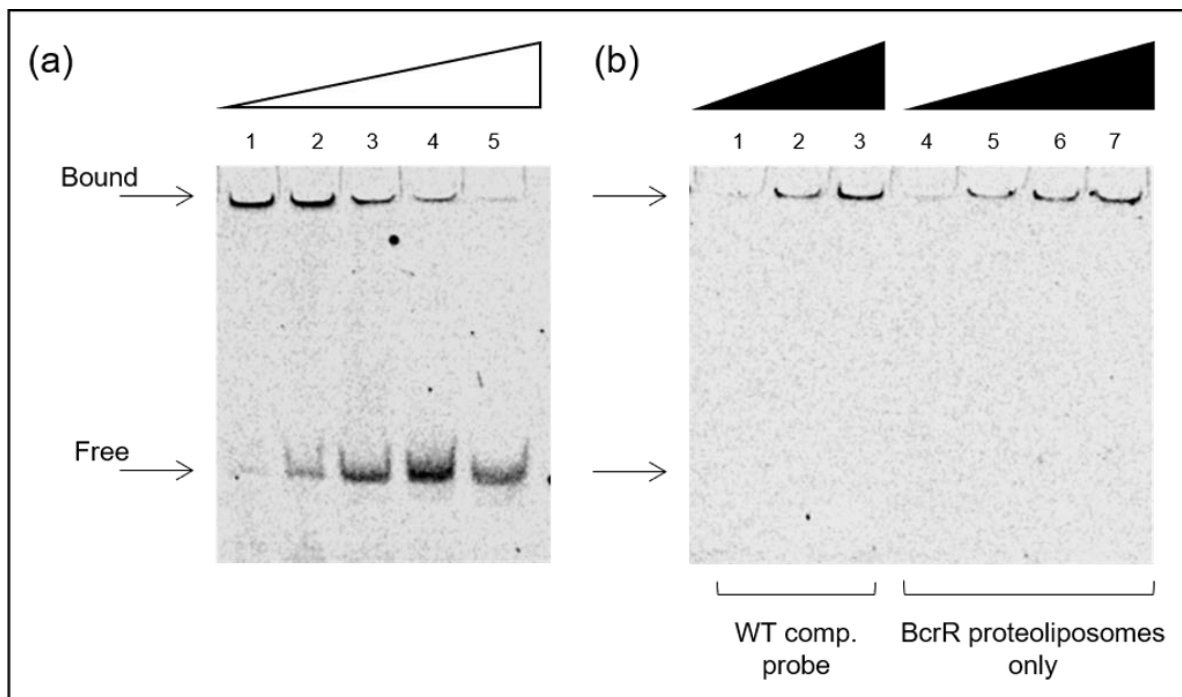


**Fig. S6. EMSA competition and controls for BcrR WT and  $P_{bcrA}$  target probe.** (a) Wild-type (WT) BcrR proteoliposomes (P/L) were incubated with a fluorescently labelled  $P_{bcrA}$  target probe and at increasing molar ratios of a non-labelled:labelled probe (5:1, 10:1, 20:1, 30:1, and 40:1) (lanes 1 – 5). The competitor probe was the same length and nucleotide sequence as the labelled target probe (see methods). Labelled probe and BcrR (proteoliposomes) were at a constant concentration of 1.25 ng and 400 ng, respectively. Fluorescently labelled bound probe was displaced at increasing concentrations concurrent with increasing non-labelled competitor probe. (b) Non-labelled competitor probe (1.25 ng) was incubated with increasing molar ratios of WT BcrR proteoliposomes (protein:DNA; 0:1, 50:1, and 125:1) (lanes 1 – 3). This confirmed the non-labelled competitor probe does not fluoresce. BcrR proteoliposomes only were shown to auto-fluoresce, with fluorescence increasing as liposome concentration increased (0, 100, 200, and 400 ng) (lanes 4 – 7). Binding reactions were incubated for 30 min at room temperature and then run on a 6% native PAGE gel at 350V for 25 min and visualised at 700 nm. Data presented here are a representative of shift assays that have been repeated at least three times.

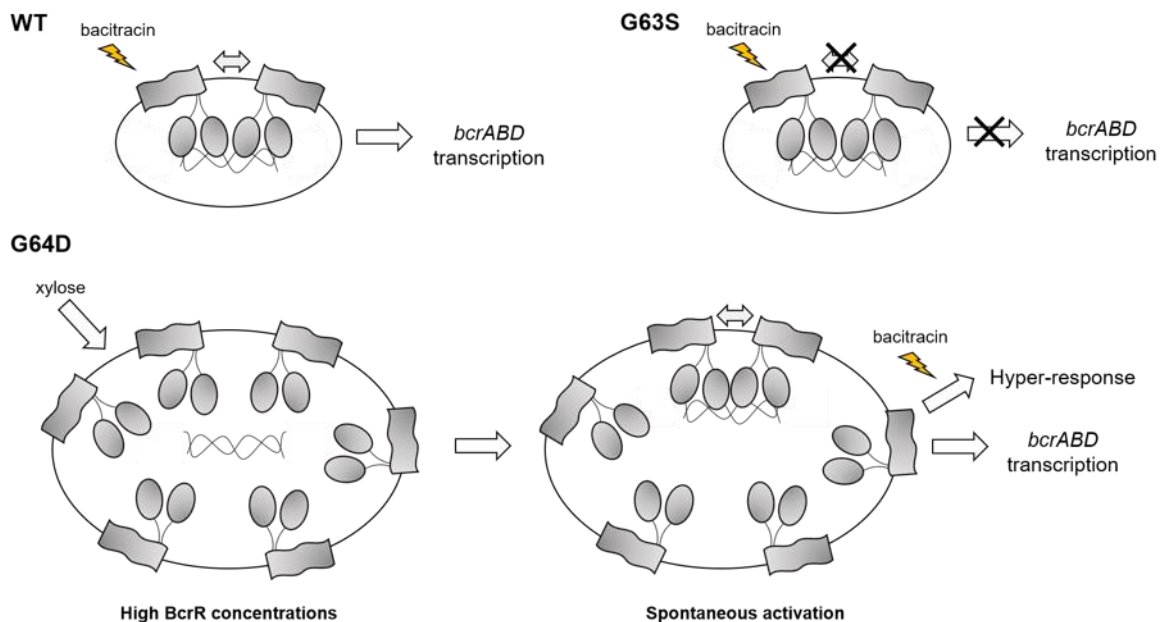


**Fig. S7. A proposed model of G64D activation.** Wild-type (WT) BcrR is constitutively bound to the *bcrA* target promoter but requires bacitracin for activation. BcrR gain of function mutant G64D can spontaneously activate and initiate expression from the *bcrA* promoter in the absence of bacitracin. This process relies upon high cellular concentrations of BcrR, as observed under a xylose-inducible promoter. In the presence of both xylose and bacitracin, G64D elicits a hyper-sensitive response as a result of spontaneous activation, in addition to bacitracin-induced activation. A G64S substitution results in a defective BcrR, unable to effectively elicit a response to bacitracin. This is likely due to an inability to oligomerise upon bacitracin-binding.

**Table S1. Bacterial strains and plasmids**

Strain or Plasmid	Description <sup>#</sup>	Reference/Source
<i>B. subtilis</i>		
SGB37	<i>bceAB::kan amyE::pES601(PbcrA-lacZ)</i> ; cm <sup>R</sup> kan <sup>R</sup>	[1]
SGB43	<i>bceAB::kan thrC::pES701(pXT-bcrR; E. faecalis)</i> <i>amyE::pES601(PbcrA-lacZ)</i> ; spec <sup>R</sup> cm <sup>R</sup> kan <sup>R</sup>	[1]
SGB273	TMB1518 <i>sacA::pNTlux101</i> ; cm <sup>R</sup>	[1]
SGB274	TMB1518 <i>thrC::pES701 sacA::pNTlux101</i> ; cm <sup>R</sup> spec <sup>R</sup>	[1]
BcrR_R11K	SGB37 harbouring pES701 BcrR <sup>R11K</sup> ; spec <sup>R</sup>	This study
BcrR_T17M	SGB37 harbouring pES701 BcrR <sup>T17M</sup> ; spec <sup>R</sup>	This study
BcrR_T30I	SGB37 harbouring pES701 BcrR <sup>T30I</sup> ; spec <sup>R</sup>	This study
BcrR_S33L	SGB37 harbouring pES701 BcrR <sup>S33L</sup> ; spec <sup>R</sup>	This study
BcrR_P42L	SGB37 harbouring pES701 BcrR <sup>P42L</sup> ; spec <sup>R</sup>	This study
BcrR_S51F	SGB37 harbouring pES701 BcrR <sup>S51F</sup> ; spec <sup>R</sup>	This study
BcrR_G64S	SGB37 harbouring pES701 BcrR <sup>G64S</sup> ; spec <sup>R</sup>	This study
BcrR_G64D	SGB37 harbouring pES701 BcrR <sup>G64D</sup> ; spec <sup>R</sup>	This study
BcrR_G88R	SGB37 harbouring pES701 BcrR <sup>G88R</sup> ; spec <sup>R</sup>	This study
BcrR_P101L	SGB37 harbouring pES701 BcrR <sup>P101L</sup> ; spec <sup>R</sup>	This study
BcrR_T123I	SGB37 harbouring pES701 BcrR <sup>T123I</sup> ; spec <sup>R</sup>	This study
BcrR_G141D	SGB37 harbouring pES701 BcrR <sup>G141D</sup> ; spec <sup>R</sup>	This study
BcrR_P180S	SGB37 harbouring pES701 BcrR <sup>P180S</sup> ; spec <sup>R</sup>	This study
BcrR_E179K	SGB37 harbouring pES701 BcrR <sup>E179K</sup> ; spec <sup>R</sup>	This study
BcrR_T183M	SGB37 harbouring pES701 BcrR <sup>T183M</sup> ; spec <sup>R</sup>	This study
BcrR_G64D_lux	SGB273 harbouring pES701 BcrR <sup>G64D</sup> ; spec <sup>R</sup>	This study

*E. coli*

DH10B	F- <i>mcrA</i> Δ( <i>mmr-hsdRMS-mcrBC</i> ) φ80 <i>lacZ</i> ΔM15 Δ <i>lacX74 deoR</i>	[2]
C41(DE3)	<i>recA1 araD139</i> Δ( <i>ara leu</i> )7697 <i>galU galK rpsL endA1 nupG</i>	[3]
C41 pTrc99A	Uncharacterised mutant derivative from BL21(DE3)	This study
WT	C41(DE3) harbouring expression vector pTrc99A; <i>amp</i> <sup>R</sup>	This study
R11K	C41(DE3) harbouring pBcrRHis <sup>WT</sup> ; <i>amp</i> <sup>R</sup>	This study
S33L	C41(DE3) harbouring pBcrRHis <sup>R11K</sup> ; <i>amp</i> <sup>R</sup>	This study
G64D	C41(DE3) harbouring pBcrRHis <sup>S33L</sup> ; <i>amp</i> <sup>R</sup>	This study
E179K	C41(DE3) harbouring pBcrRHis <sup>G64D</sup> ; <i>amp</i> <sup>R</sup>	This study
T183M	C41(DE3) harbouring pBcrRHis <sup>E179K</sup> ; <i>amp</i> <sup>R</sup>	This study

*E. faecalis*

AR01/DGVS	AR01/DG cured of pJM02 <i>bac</i> <sup>R</sup>	[4]
-----------	--	-----

*Plasmids*

pES701	pXT- <i>bcrR</i> (wild-type) <i>E. faecalis</i> ; <i>spec</i> <sup>R</sup>	[1]
pTrc99A	<i>E. coli</i> protein expression vector; <i>amp</i> <sup>R</sup>	[5]
pBcrRHis <sup>WT</sup>	pTrc99A- <i>bcrR</i> wild-type; <i>amp</i> <sup>R</sup>	This study
pBcrRHis <sup>R11K</sup>	pTrc99A- <i>bcrR</i> G33A mutation; <i>amp</i> <sup>R</sup>	This study
pBcrRHis <sup>S33L</sup>	pTrc99A- <i>bcrR</i> C98T mutation; <i>amp</i> <sup>R</sup>	This study
pBcrRHis <sup>G64D</sup>	pTrc99A- <i>bcrR</i> G192A mutation; <i>amp</i> <sup>R</sup>	This study
pBcrRHis <sup>E179K</sup>	pTrc99A- <i>bcrR</i> G535A mutation; <i>amp</i> <sup>R</sup>	This study
pBcrRHis <sup>T183M</sup>	pTrc99A- <i>bcrR</i> C548T mutation; <i>amp</i> <sup>R</sup>	This study

---



1. **Fang C, Stiegeler E, Cook GM, Mascher T, Gebhard S.** *Bacillus subtilis* as a platform for molecular characterisation of regulatory mechanisms of *Enterococcus faecalis* resistance against cell wall antibiotics. *PLoS One* 2014;9:1–10.
2. **Hanahan D, Jessee J, Bloom FR.** Plasmid transformation of *Escherichia coli* and other bacteria. *Methods Enzymol* 1991;204:63–113.
3. **Miroux B, Walker JE.** Over-production of proteins in *Escherichia coli*: Mutant hosts that allow synthesis of some membrane proteins and globular proteins at high levels. *J Mol Biol* 1996;260:289–298.
4. **Manson JM, Keis S, Smith JMB, Cook GM.** Acquired bacitracin resistance in *Enterococcus faecalis* is mediated by an ABC transporter and a novel regulatory protein, BcrR. *Antimicrob Agents Chemother* 2004;48:3743–3748.
5. **Amann E, Ochs B, Abel KJ.** Tightly regulated tac promoter vectors useful for the expression of unfused and fused proteins in *Escherichia coli*. *Gene* 1988;69:301–315.